NASA Technical Memorandum 101989

NASA's Program on Icing Research and Technology

John J. Reinmann, Robert J. Shaw,
and Richard J. Ranaudo
Lewis Research Center
Cleveland, Ohio

Prepared for the
Symposium on Flight in Adverse Environmental Conditions
sponsored by the Flight Mechanics Panel (FMP) of AGARD
Gol, Norway, May 8–12, 1989

NASA

NASA'S PROGRAM ON ICING RESEARCH AND TECHNOLOGY

John J. Reinmann, Robert J. Shaw and Richard J. Ranaudo
National Aeronautics and Space Administration
Lewis Research Center
Cleveland, Ohio 44135 U.S.A.

SUMMARY

This paper reviews NASA's program in aircraft icing research and technology. The program relies heavily on computer codes and modern applied physics technology in seeking icing solutions on a finer scale than those offered in earlier programs. Three major goals of this program are (1) to offer new approaches to ice protection, (2) to improve our ability to model the response of an aircraft to an icing encounter, and (3) to provide improved techniques and facilities for ground and flight testing. This paper reviews the following program elements: (1) new approaches to ice protection; (2) numerical codes for deicer analysis; (3) measurement and prediction of ice accretion and its effect on aircraft and aircraft components; (4) special wind tunnel test techniques for rotorcraft icing; (5) improvements of icing wind tunnels and research aircraft; (6) ground deicing fluids used in winter operation; (7) fundamental studies in icing; and (8) droplet sizing instruments for icing clouds.

INTRODUCTION

The icing problem is receiving more attention today than it has in any other period of the last 25 years. For example, at the NASA Lewis Research Center, testing activity in the Icing Research Tunnel (IRT) has increased steadily over the past 10 years, and in 1988 the IRT logged 1330 hr of test time, which is the highest annual usage on record since 1950.

There are many reasons for the current interest in icing: (1) the more efficient, high by-pass ratio engines of today and the advanced turboprop engines of tomorrow have limited bleed air for ice protection, so the airframers are seeking more efficient systems; (2) airfoil designers do not want their
modern, high-performance surfaces contaminated with ice, so they are intensifying pressure to develop ice protection systems that minimize residual ice and thereby allow the airframer to keep airfoil surface area to the minimum; (3) new military aircraft requiring all-weather capability are currently under development; (4) some existing military aircraft, being used primarily for training missions, are experiencing foreign object damage (FOD) due to icing conditions they would not normally encounter in combat; (5) designers of high performance military aircraft want to avoid burdening the aircraft with ice protection, so they want to know where and how much ice will build on the aircraft and whether the aeroperformance penalties are acceptable; (6) designers of future high performance aircraft with relaxed static stability need to know how their aircraft will perform with contaminated aerodynamic surfaces; (7) little is known about the effects of ice accretion on the operation and performance of advanced turboprops, and whether or not ice protection will be required; and (8) the FAA has certified only one civilian helicopter for flight into forecasted icing, which implies a strong need for support of helicopter icing.

NASA's icing program was first reviewed in 1983 (Ref. 1). Many elements of the early program are still in progress, and they are brought up to date in this paper. Some new elements have been added, the most notable ones being the following: ice protection systems based on electro-mechanical impulses; effects of ground deicing fluids on wing aerodynamic performance during takeoff; upgrades and enhancements to the LEWICE ice accretion prediction code; applications of viscous flow codes to the icing problem; experimental observations of the ice accretion process; and structural and adhesive properties of impact ice.

Other review articles have been published on parts of the NASA aircraft icing program. Reference 2, published in 1984, gave an account of our aircraft icing analysis activities (analytical and experimental). Several review papers (Refs. 3 to 5) were published in 1988. Reference 3 gave an update of our icing analysis activities for ice accretion on unprotected airfoils. Reference 4 reviewed our analytical modeling, wind tunnel experiments, and flight testing and showed how they support our goal of modeling the effect of icing on the whole aircraft. Reference 5 reviewed the numerical codes that model the transient performance of electrothermal deicing systems.

This paper attempts to present the full scope of NASA's extensive program in aircraft icing research and technology. Three major goals of this program are (1) to offer new approaches to ice protection, (2) to improve our ability to model the response of an aircraft to an icing encounter, and (3) to provide improved techniques and facilities for ground and flight testing.

For several years, the Federal Aviation Administration (FAA) has contributed financial support to the NASA icing program, especially in the areas of ice accretion modeling, cloud droplet instrumentation evaluation and calibration, and icing scaling.

ICE PROTECTION SYSTEMS

Since the mid 1950's, jet transports have kept their critical lifting surfaces and engine inlets completely clear of ice by employing hot air anti-icing systems. But more recently, as jet engine manufacturers have begun increasing engine by-pass-ratios to achieve higher efficiencies, the engine cores have become smaller and the amount of hot bleed air available for anti-icing has shrunk significantly (Fig. 1). To cope with this loss of bleed air, airframers are (1) eliminating ice protection from selected components, or (2) developing the more energy-efficient deicing systems that require some buildup of ice before activation. Helicopters, general aviation, and light transport aircraft, all with relatively small payload fractions and low power margins, have always relied heavily on the more efficient deicing systems.

Always in demand are new ice protection systems that can offer any of the following improvements: lower weight, lower power consumption, more effective ice removal, more reliable operation, more easily retrofitted to existing components, smaller aero penalties, lower maintenance costs or lower manufacturing costs. NASA has selectively supported the development of ice protection systems, with emphasis on the more efficient deicing systems.

Next to pneumatic deicer boots, the most efficient mechanical deicing systems are those that employ electro-mechanical impulses. Typically, the power

required for electro-mechanical deicing is about one percent of that used for evaporative anti-icing. Electro-mechanical deicers use about as much power as the aircraft's landing lights.

Three deicing systems employing electro-mechanical impulses have been supported by NASA. These are (1) the Electro-Expulsive Separation System (EESS), (2) Electromagnetic Impulse Deicers (EIDI), and (3) Eddy Current Repulsion Deicer Boots (ECRDIB). All three of these systems are energized by rapidly discharging a capacitor through electrical conductors whose currents set up opposing magnetic fields that force the conductors rapidly apart. The short discharge pulse, a fraction of a millisecond in duration, imparts an impulsive force to the ice that shatters, debonds, and expels it from the surface. The required power supplies and switching circuitry are nearly identical for the three systems.

Electro-Expulsive Separation System

The EESS system was invented and patented by Mr. L. A. Haslim of the NASA Ames Research Center, Moffett Field, CA (U.S. Patent No. 4,690,353; September 1, 1987). Though it has undergone only limited icing testing to date, it appears to be an effective deicer. It seems to be especially effective for removing thin layers of ice. Thus the EESS can be activated after very thin layers of ice have built up, which should minimize the aeroperformance penalties caused by ice accumulated between activations or by residual ice left after activation. Because it can be easily manufactured as a thin boot and easily retrofitted by bonding to the outside of any component, several companies are interested in applying it to both civilian and military aircraft.

As shown in Fig. 2 the EESS conductors are arranged as a series of U-shaped ribbons such that the current flows into one leg of the U and out the other. When the capacitor discharges into the ribbon, the opposing currents in the two legs create opposing magnetic fields that force adjacent ribbons rapidly apart. The conductors are embedded in the elastomeric boot as shown in Fig. 3. Slits in the deicer boot allow the ribbon conductors to move rapidly apart and then they quickly collapse back to a thin layer.

The B. F. Goodrich Company tested the EESS system on board the NASA Twin Otter icing research aircraft, and Data Products of New England tested it in the NASA IRT. and on the Twin Otter.

Through a competitive bidding process, NASA has granted limited patent rights for the EESS to Data Products of New England, Wallingford, CT. Reference 6 provides a discussion of the improvements that Data Products of New England is currently carrying out on the EESS.

Data Products of New England offers blankets from 0.040 to 0.080 in. thick, smooth on both sides, and capable of being feathered into the surface on which they are installed. Thickness adds durability, but reduces blanket efficiency and may affect air flow. Blankets weigh between 0.7 and 1.1 lb/ft^2. Each rectangular area of approximately 70 $in.^2$ maximum is connected to one Blanket Driver Assembly (i.e., a capacitor and related switching circuitry). Five separate blankets were pulsed for a total of 50 000 cycles, with greater than 10 000 cycles being the highest on one blanket, with no discernible degradation.

Electromagnetic Impulse Deicer

NASA recently completed a development program on the EIDI system that began in 1982. Reference 7 is the final EIDI report that summarizes the program history, test results, technical accomplishments, and analysis and design procedures for the implementation of an EIDI system.

The physical form of the EIDI method is shown in Fig. 4. Flat-wound coils made of copper ribbon wire are placed just inside the leading edge of a wing's skin with a small gap separating skin and coil. Either one or two coils are placed at a given span wise station, depending on the size and shape of the leading edge. Two methods of supporting coils are shown: support by a front spar or from a beam attached to ribs is generally used, but mounting to the skin itself is sometimes used.

Energy is discharged from a capacitor through the EIDI coil. The rapid discharge creates a rapidly forming and collapsing electromagnetic field which induces eddy currents in the metal skin. The magnetic fields resulting from current flow in the coil and skin create a repulsive force of several hundred pounds magnitude, but a duration only a fraction of a millisecond. A small amplitude, high acceleration movement of the skin acts to shatter, debond and expel the ice. Two or three such "hits" are performed sequentially, separated by the time required to recharge the capacitors, then ice is permitted to accumulate until it again approaches an undesirable thickness.

Deicing has been successfully accomplished in the icing wind tunnel and in flight for typical general aviation and transport wings and inlet nacelles under a wide range of velocities, angles of attack, icing rates and temperatures. Testing consisted of eleven sets of icing tunnel tests and two flight test programs. Fatigue tests were conducted for the wing skin and the EIDI components. Tests on electromagnetic interference (EMI) with other aircraft systems was also conducted. Both fatigue life and EMI emissions can be made acceptable.

EIDI's major advantage is that it does not alter the external surfaces of the aircraft, and therefore does not impose an aerodynamic performance penalty. Its limitation is that it does not adapt readily to retrofitting, since in most cases it must be considered a part of the original design of the component. The fundamental technology for EIDI is now established, and it is up to the various airframers and engine nacelle fabricators to adopt it. Those who have worked on the EIDI program are convinced that it is just a matter of time until it makes its way onto a next generation aircraft.

Eddy Current Repulsion Deicing Boot

The ECRDIB contains electrical conductors in an elastomeric boot that is bonded to the leading edge of a wing. When a capacitor is discharged through the conductors, eddy currents are induced in the skin of the wing, just as in EIDI. Opposing magnetic fields repel the boot rapidly away from the wing. We say that ECRDIB is EIDI applied on the outside rather than the inside of the wing. (ECRDIB differs from EESP in that EESP does not induce eddy currents.) NASA has a small contract with Electroimpact, Inc., Seattle, WA, to fabricate several ECRDIB units and test them on a large-chord and a small-chord wing section in the NASA IRT.

The ECRDIB conductors will be fabricated from stacks of thin, flexible circuit boards, with a coil conductor pattern that allows current to enter and exit the edge, rather than the center, of the circuit board. A sheet of elastomeric material will cover the circuit boards to form the boot. The inventor (Ref. 8) has calculated that for the same pulse of energy, the ECRDIB should deice about two to four times the area an EESS would deice.

The EESS and the ECRDIB systems are embedded in elastomeric boots that are applied over the outside of the airfoil. As with the pneumatic boot, these elastomeric outer surfaces will tend to get pulled away from the airfoil skin in the region of negative pressures or suction pressures, i.e., on the upper leading edge of the airfoil. This would cause upper surface distortion and an attendant aerodynamic performance penalty. Designers of pneumatic boots pull a vacuum on the inside of the boot to prevent the boot from staying inflated after the boots are activated. Pulling a vacuum on an EESS or ECRDIB seems impractical, and some other means must be found to overcome this problem. Data Products appears to have solved this problem for EESS.

The other issue with elastomeric materials is their ability to withstand rain and sand erosion. Erosion would be most serious near the outboard sections of helicopter rotors. Perhaps an acceptable solution for rotors would be a hybrid system consisting of EESS on the inboard sections and electrothermal on the outboard sections.

PREDICTIONS OF AIRFOIL AERODYNAMIC PERFORMANCE DEGRADATION DUE TO ICING

A major goal of the NASA aircraft icing program is to develop and experimentally validate a group computer codes that will predict the details of an aircraft icing encounter. The flowchart in Fig. 5 shows the many codes required to form such an overall icing analysis methodology and indicates the codes currently under development by NASA. Once validated, these codes can be used for (1) preliminary design studies to ascertain component sensitivity to icing, (2) performance predictions of proposed ice protection systems, (3) computer-based certification or qualification studies to reduce the amount of required icing flight testing, and (4) more realistic icing effects inputs for use in flight training simulators.

This section will review the progress on one goal of the overall activity, namely, to produce codes that predict the ice buildup on an unprotected airfoil and the resulting aerodynamic degradation. NASA has given the name LEWICE to its overall ice accretion code. (This section is a condensation of the material in Ref. 3 and also includes some more recent material).

Figure 6 illustrates the aerodynamic performance penalties caused by leading edge ice: (1) increased drag even at low angles-of-attack; (2) airfoil decambering due to a thickened upper surface boundary layer; and (3) reduced $C_{l_{max}}$ and premature stall due to separation of the airfoil upper surface boundary layer.

Overall Approach

Figure 7 shows the key physical processes that must be adequately modeled in any airfoil icing analysis methodology. In the LEWICE approach, ice is

grown layer by layer, where each layer represents the ice accretion for one user-specified time increment. The overall approach for LEWICE is as follows: (1) a potential flow code calculates the flow field around the airfoil; (2) a droplet trajectory code, using the inviscid flow velocities, computes the local water flux around the airfoil; and (3) an ice accretion code, using the local water fluxes and inviscid velocities, calculates the local ice growth around the airfoil. At this point the code can loop back and re-run the potential flow analysis to determine the new inviscid flow field around the iced airfoil. Then a new droplet trajectory calculation and a new ice accretion calculation can be completed for the second time step, and so on. The looping process is repeated for as many time increments as required to reach the overall icing encounter time. If aerodynamic performance losses are required for the iced airfoil, then a viscous flowfield calculation is performed for the predicted ice shape.

It is highly desirable to replace the separate inviscid and viscous flow calculations with a single viscous flow calculation. However, we have not yet made the replacement because a viscous flow calculation requires far more computer time than does an inviscid calculation, so the total CPU time to calculate an ice shape would be impractical for routine calculations. Obviously as the ice shape grows and dominates the airfoil leading edge flowfield, viscous effects (boundary layer separation and reattachment) will become so important that the simplified inviscid analysis will no longer be appropriate.

The following sections will look at the modules in more detail.

Inviscid Flowfield/Droplet Trajectories

The inviscid flowfield code is a second order panel code. Droplet trajectories are obtained by integrating Newton's second law of motion using a predictor-corrector scheme optimized for stiff systems of equations.

An experimental droplet impingement data base is being obtained for use in validating the droplet trajectory prediction codes (Ref. 3). Comparisons between analysis and experiment are shown in Fig. 8. The comparisons show that the prediction, when using either inviscid or viscous flowfield velocities, is quite accurate for cases of small ice accretion, but not as accurate for large ice accretions that have massive flow separation with unsteady flow. Figure 8 shows that while the predicted collection efficiencies were lower when the viscous flow velocities were used in the trajectory calculations, they were not as low as those observed in the experiment. Since the Navier-Stokes codes overpredicts the velocities near the separation points, the next logical step seems to be to replace the actual model geometry with a geometry that follows the outer boundary of the separated flow region behind the horns. This geometry should not produce the higher velocities near the beginning of separation, and should begin turning the flow further upstream, thereby reducing the droplet collection efficiency. We plan to try this in the near future.

Ice Accretion

The ice shape module predicts ice shapes by solving the continuity and energy equations for differential control volumes on the surface of the airfoil as depicted in Fig. 9. The code determines the fraction of incoming water

that freezes in each control volume. Any water that does not freeze in a control volume is assumed to flow back to the immediately aft control volume.

Figure 10 shows representative comparisons of predicted shapes versus actual ice shapes grown on a NACA 0012 airfoil in the NASA IRT. The agreement in predicted versus measured ice shape for both the rime and glaze ice was judged to be acceptable. Typically, LEWICE predicts rime ice shapes very well, but it can have difficulty with glaze ice predictions. Other comparisons with in-flight icing are given in Ref. 9.

The dependence of airfoil drag on ice formation temperature is shown in Fig. 11 (Ref. 10). Notice that at the warmer temperatures the drag is extremely sensitive to ice formation temperature. Also note that the mass of accreted ice stays relatively constant until the temperature approaches the freezing point of water, and then the mass drops off, presumably because the runback water blows off the airfoil. The current NASA ice accretion module does not account for water blowoff.

A key part of the ice accretion module is the method used to predict heat and mass transfer convection coefficients. The convection coefficients are calculated by the integral boundary layer method (Ref. 3). The ability to model surface roughness as an equivalent sand grain roughness is an important feature of the integral boundary layer method. The predictions were compared with results from a heat transfer experiment in which ice shapes grown on a cylinder in the IRT were replicated in a wood model that was instrumented with surface heat flux gauges (Ref. 11). The predicted heat transfer coefficients shown in Fig. 12 do not agree favorably with the experimental data.

Figure 13 compares the experimental data with predictions made with a Navier-Stokes code that solves the energy equation and uses a distributed roughness model (Ref. 12). The agreement between analysis and experiment is good.

The icing process modeled in LEWICE follows closely the model given by Messinger (Ref. 13). The Messinger model, as depicted by Olsen (Ref. 14), is shown in Fig. 14. Olsen took closeup movies of the actual ice accretion process under a variety of ice formation conditions in the IRT, and his observations lead him to propose the new model shown in Fig. 15. In this model, water flows along the surface only during the initial moments of exposure to the icing cloud. After that, the water begins to form beads on the surface as shown in Fig. 16. Ice forms in the base of the beads and impinging water accumulates at the top of the beads.

Hansman (Refs. 15 and 16) later followed up on Olsen's work and basically confirmed Olsen's observations. Hansman observed several distinct zones of surface water behavior: a smooth wet zone in the stagnation region with a uniform water film; a rough zone where surface tension effects caused coalescence of surface water into stationary beads; a horn zone where roughness elements grew into horn shapes; a runback zone where surface water ran back as rivulets; and a dry zone where rime feathers formed. The location of the transition from the smooth to the rough zone was found to migrate with time towards the stagnation point. The behavior of the transition appeared to be controlled by boundary layer transition and bead formation mechanisms at the interface between the smooth and rough zones. Regions of wet ice growth and enhanced heat transfer were clearly observed with infrared video recordings of glaze ice surfaces.

Hansman formulated a three zone model and tested it by forcing the LEWICE ice accretion module to have three zones. A zone near the stagnation region was modeled by the original control volume approach. A second zone was modeled as freezing all the water that impinged on it. A third zone was modeled as a transition zone separating the other two zones. In the transition zone the control volumes had freezing fractions that varied linearly from the value at the edge of the first zone to a value of unity at the edge of the second zone. Figure 17 shows how an experimental ice shape formed on a cylinder compared with the predictions made by the unmodified approach and by the Hansman approach. Hansman's model gave results far superior to the unmodified approach.

Because this new multi-zone model holds promise of being more representative, NASA will continue to conduct fundamental experiments on the details of the ice accretion process, such as, closeup movies in natural icing clouds and infrared studies of the surface of the ice (Ref. 16)

Aerodynamic Performance

As noted earlier, it is highly desirable to replace the potential flow code in LEWICE with a viscous flow code that more accurately models the flowfield and also allows a direct calculation of lift, drag, and pitching moment. To this end, NASA is developing two viscous flow codes: (1) a Reynolds averaged thin layer Navier-Stokes code (ARC2D) (Ref. 17), and (2) an interactive boundary layer code (IBL) (Ref. 18). Both of these codes were designed to handle clean airfoils and are being extended to handle iced airfoils for which flow separation and reattachment at lower angles-of-attack is not uncommon. The IBL code is attractive for inclusion in LEWICE because it utilizes a potential flow code which requires far less computer power than the Navier-Stokes code.

A comprehensive experimental data base for validating the viscous flow codes is being developed as Fig. 18 illustrates. A NACA 0012 airfoil model was modified to have a leading edge ice shape that had the gross cross sectional features of an ice shape grown in the IRT, but also had a geometry that could be accurately digitized to allow inputting to flow analysis codes.

Figure 19 compares the predictions of the ARC2D and IBL codes with the experimental data base described by Fig. 18. At lower angles-of-attack, both codes compared well with experiment. At the higher angles-of-attack the IBL code underpredicted the measured drag levels. At these higher angles the ARC2D code predicted unsteady flow. Although the IBL code appeared inadequate at the high alphas for this case, Cebeci (Ref. 19) showed that the IBL code can do a good job on clean airfoils beyond stall.

NASA is supporting grid definition studies (Ref. 4) and also developing an adaptive grid generation code that should prove useful for generating a new grid for each new time step in the LEWICE ice accretion calculation. Another supporting effort for the ARC2D code is the testing of various turbulence models such as the Baldwin-Lomax model and the Johnson-King model, as well as a model developed in-house (Ref. 20).

Work is continuing on improving the two-dimensional viscous flow codes and on conducting experiments to validate them. The next step is to begin work on three-dimensional codes for application to modern swept-wing aircraft. To

this end, NASA is conducting wind tunnel testing at the Ohio State University (Ref. 21) on three-dimensional rectangular and swept semi-span wings with and without attached ice shapes. A data base similar to the two-dimensional data base (see Fig. 18) will be acquired. NASA is also supporting development of a three dimensional Navier-Stokes code (Ref. 22) that will be validated against the experimental data.

Although a great deal of research still needs to be done on ice accretion modeling and aeroperformance penalties, the codes presented in this section are representative of the best available at this time. Many organizations in the U.S.A. are using these codes as research codes and are relaying their experiences with them to NASA and its grantees and contractors.

AIRPLANE PERFORMANCE AND STABILITY AND CONTROL CHANGES DUE TO ICING

Since ice will accumulate on selected surfaces of modern aircraft, and since failure of any ice protection system will result in ice accumulations, NASA has a major program element to study the effects of icing on aircraft performance and stability and control. The approach employs three interrelated elements: analysis, wind tunnel experiments, and considerable flight testing in natural icing clouds.

In the previous section, we reviewed NASA's research on the effects of icing on airfoil aerodynamics. In this section we will concentrate on flight testing in natural icing clouds.

Research Aircraft

The NASA Lewis icing research aircraft shown in Fig. 20 is a modified DeHavilland DH-6 Twin Otter (Refs. 23 to 25). The aircraft is equipped with electrothermal anti-icers on the propellers, engine inlets, and windshield. Pneumatic deicer boots are located on the wing outboard of the engine nacelles, on both the horizontal and vertical stabilizers, on the wing struts, and on the rear landing gear struts. The pneumatic deicers located on the vertical stabilizer, wing struts, and landing gear struts are nonstandard items that provide additional research capability for measuring component drag through selective deicing. The aircraft is equipped with several standard instruments for measuring icing cloud properties (Ref. 26).

Wing leading edge ice shapes are measured in flight with a stereo photography system. Wing section drag is measured with a wake survey probe mounted on the wing behind the region where the stereo photos are taken. A noseboom is used to measure airspeed, angle-of-attack, and sideslip.

A complete flight test system is being built up to measure flight dynamics along a flight path. The system will include a data acquisition system and an inertial package that contains rate gyros, directional gyros, and servo accelerometers.

Wing Ice Shapes and Drag

One purpose of the icing flight research program is to obtain inflight data that can be used to validate computer codes and to confirm that the NASA Lewis Icing Research Tunnel adequately simulates natural icing. We have flown numerous flights through natural icing clouds, in which ice was allowed to build up on the wing leading edge. The aircraft was then flown out of the cloud into clear air, where stereo photographs were taken of the ice shape and a drag wake survey probe was moved across the trailing edge of the wing behind the ice shape (Ref. 24). Figure 21 shows the ice shape derived from the stereo photos and Fig. 22 shows the increase in drag versus angle-of-attack.

Later this year, a section of a Twin Otter wing will be mounted in the IRT (Fig. 23), and ice shape and drag will be measured under the same conditions as in flight so that a direct comparison can be made between flight and the IRT.

Aircraft Performance

Airframe icing degrades aircraft performance by reducing lift and increasing drag. This results in higher stall speeds, lower angles-of-attack for stall, lower climb, lower cruise, and lower power margins for engine out performance. These performance degradations were measured on the icing research aircraft for a wide range of icing conditions. By deicing one airframe component at a time and taking a set of performance measurements after each deicing event, we obtained lift loss on the wing and relative values of drag increase for each airframe component. For some cases power required versus power available was measured to assess the effects on engine-out performance (Ref. 27).

Results from a flight in glaze icing conditions (Ref. 27) are shown in Fig. 24. The most noticeable changes in the lift curves due to ice are lower slopes and reduced $C_{l_{max}}$. The test aircraft has a $C_{l_{max}}$ of approximately 1.4 in the clean, no flap configuration. With ice, $C_{l_{max}}$ is reduced to something less than 1.0. The loss in lift that remains after deicing all components is largely because the portion of the wing between the engine nacelles and fuselage has no ice protection. Another factor, more difficult to evaluate, is the contribution to lift loss made by residual ice left on the wings after cycling the deicer boots.

Figure 24 also shows the drag increase due to airframe icing. To a pilot, this translates into degraded aircraft performance, especially in the event of an engine-out condition. Figure 25 shows the relationship between power required and power available under the glaze icing conditions. The increase in power required means lower climb rates, altitude potential, and cruise speeds. These factors become essential for the pilot to consider when planning his options under an engine-out condition.

Stability and Control

NASA is formulating a methodology that will predict the effect of ice accretions on the stability and control characteristics of aircraft. This methodology will be useful in aircraft design, safety and airworthiness analyses, flight control system design for relaxed static stability aircraft, and possibly in providing simulator software for pilot training.

Rather limited flight tests have been conducted so far. These tests were structured to determine whether the icing effects were measurable, and if so, what their values were. The stability and control flight tests investigated only the longitudinal characteristics (Ref. 25 and 28). For these tests the icing research aircraft was configured with a Styrofoam layer of simulated ice bonded to the leading edge of the horizontal tail as shown in Fig. 26.

The flight test maneuvers and data acquisition were designed to provide a statistically significant ensemble of data points that could be analyzed by a Modified Stepwise Regression (MSR) technique to yield estimates of the stability and control derivatives. The aircraft was flown in the clean (baseline) configuration and then later with the "Styrofoam ice" on the horizontal tail. Forty five repeat maneuvers were flown at identical conditions for each configuration.

The MSR technique (Refs. 28 and 29) accurately estimated the longitudinal stability and control derivatives throughout the flight envelope of the aircraft. Figure 27 shows how elevator control power was degraded over the range of attainable flight speeds at a constant power setting. Note that the estimated variations, or predicted bands of uncertainty, were less than the measured changes.

In a supporting analytical effort, the icing research aircraft geometry was paneled up for input to a three dimensional airflow code (VSAERO). The digital description included propellers and both the baseline and iced-tail geometry. The ARC2D (Ref. 17) code was also run to obtain a modified geometric definition of the iced tail for input to VSAERO. The initial VSAERO calculations predicted nearly the same decrease in stability due to ice as the flight test did. However, the calculated results also indicated that the nonlinear downwash due to the propeller must be better modeled in VSAERO to obtain the correct power effects.

ROTORCRAFT ICING RESEARCH

Helicopter companies use the NASA IRT and other icing tunnels for testing engine inlets, rotor ice protection systems on a stationary rotor blade (i.e., no centrifugal force), stabilators, external stores, weapons systems, optical systems, velocity sensors, and other vulnerable parts of a helicopter. However, a full-scale, rotating main rotor will not fit into any known icing wind tunnel. Therefore, to prove that the main rotor and tail rotor can operate successfully in icing, manufacturers have no choice but to fly their helicopters in icing clouds.

Because helicopters are slow and have a short range, they must wait for the weather to come to their home base of operations. This dependence on local weather further aggravates the most difficult icing certification problem: finding clouds that cover the wide range of natural icing conditions required for certification -- a range that often seems unattainable due to the low probability of some of the conditions. Thus it requires years to acquire enough icing data for either FAA certification or military qualification. Since U.S. helicopter manufacturers want all-weather operational capability and want to overcome this heavy dependence on flight testing, NASA has been working with them to develop an icing test capability for sub-scale helicopter rotors in the NASA IRT.

Model Rotor Testing in the NASA Icing Research Tunnel

We have recently completed an icing test of a rotating OH-58 tail rotor in the IRT. The OH-58 tail rotor has a 13.3 cm chord and a 1.57 m diameter. The primary purpose of this test was to develop the techniques for operating a model rotor in an icing wind tunnel. The secondary purpose was to acquire data for use in developing various computer codes that predict ice accretion, ice shedding, and rotor performance degradation due to ice on rotors.

Operational concerns addressed in the test program were as follows: model and tunnel startup; coordination of model and tunnel operation; model and tunnel shutdown; observation and documentation of the rotor ice accretion and shedding; safety and emergency procedures; reaction of the rotor to the accretion and shedding of ice, and the control of the model under these circumstances.

Video cameras recorded overall and closeup views of the rotor ice buildup and shedding processes. A remotely controlled 35-mm camera was also used for detailed photographs of the ice formations during the runs. After each run, photographs and tracings of the ice shapes were taken for each blade. For some selected ice shapes, molds were made from which castings of the ice will eventually be made.

A substantial and unique rotor ice accretion and performance data base was acquired in this test. The rotor blade ice shapes were found to be quite repeatable for a given set of conditions, and corresponding iced rotor torque values were also repeatable up to the onset of shedding. When ice did shed, the inboard radial extent from which ice never shed was relatively repeatable, but the shed times, locations, and quantities of ice shed varied substantially from run to run. Although considered preliminary, this data will be useful for comparisons with the predictions of ice accretion codes, rotor performance codes, and ice shedding models.

Figures 28 and 29 show photos of the OH-58 tail rotor rig and of ice accretions on the rotor, and Fig. 30 shows rotor torque versus time during a typical icing encounter. A detailed report of these tests is in preparation and will be published as Ref. 30.

The successful test of the OH-58 tail rotor has prepared the way for a more sophisticated model rotor test that will be run in the IRT later this year. In this test, a scale model of the UH-60 Blackhawk (Fig. 28) will be tested with four NACA 0012 rotor blades, and data will be acquired with a six-component force balance. All four major U.S. helicopter companies will participate in the test.

ADVANCED TURBOPROP ICING STUDIES

NASA Lewis Research Center has been the U.S. leader in managing the development of the new high speed, high efficiency aircraft propulsion system, called the advanced turboprop (ATP). The ATP can operate efficiently up to about 0.85 Mach numbers. One of the ATP technology issues that requires research is ice protection (Ref. 31). Although aircraft equipped with advanced turboprops will cruise at altitudes above the FAR Part 25 Appendix C icing

envelopes, they are expected to encounter icing conditions during ground operation, take-off, climb, descent, low altitude hold, and they may cruise with accreted ice obtained at the lower altitudes. Of primary concern is the potential performance degradation of ATP's in icing environments. Advanced turboprops are built so ruggedly that it is unlikely that asymmetrical ice sheds will pose a serious vibration problem, if any at all.

Whether the ATP will require ice protection is not known yet. At warmer icing temperatures, it is likely that the ice can be shed from the turboprop blades by simply increasing engine rpm. But the ice may not shed at the coldest icing temperatures where ice adhesion is known to be stronger. Even if the ice can be shed at the coldest temperatures, some residual ice may cling to the blades and cause a loss in lift and an increase in drag.

To study the effect of ice accretion on ATP performance, NASA, Hamilton Standard, and Pratt & Whitney jointly conducted an icing test program at the Fluidyne Icing Tunnel (Ref. 31). The testing consisted of evaluating the ice accretion characteristics and resulting aerodynamic degradation for two thin, two-dimensional airfoil sections that were representative of advanced turboprop airfoils. The tests were conducted over a wide range of icing conditions, angles-of-attack, and Mach numbers (0.3 to 0.8). At each test point, the accreted ice shape and weight were recorded. Airfoil drag and surface pressures were measured for each run.

This data can be used for several purposes: (1) to compare with LEWICE predictions of ice shape; (2) to compare with lift and drag predictions in the literature; (3) for predicting ATP performance in icing; and (4) for constructing a composite ice shape that could be bonded to the leading edge of ATP blades for measuring performance losses during flight.

Other proposed efforts under consideration for the longer term include testing of a scale-model ATP in the IRT. The goals of these tests would be (1) to measure performance changes due to icing, (2) record actual ice accretion shapes, (3) observe shedding characteristics, and (4) use the resulting data to validate propeller performance codes and ice shedding codes. It is unlikely that satisfactory icing scaling laws will be found for relating sub-scale model testing to full-scale. But if the sub-scale data can be used to develop fundamental computer models for predicting changes in performance and ice shedding characteristics, we may be able to bypass the scaling question and use these models to predict full-scale results.

GROUND DEICING FLUIDS FOR WINTER OPERATION

The Boeing Commercial Airplanes Company and NASA conducted a joint test program in the IRT to evaluate the Type I and Type II ground deicing fluids that are used by the Association of European Airlines (AEA) during winter operations (Ref. 32). Several experimental fluids were also tested as possible candidates to replace the then-current Type II fluids. The object of the tests was to assess the aerodynamic performance penalties that result when an airplane takes off with ground deicing fluids on its wings.

Type I fluids are propylene glycol, which have hold times similar to those of the ethylene glycol fluids used in the U.S.A. for removing ice and

snow from aircraft prior to takeoff. Type II fluids are non-Newtonian (thixotropic) fluids whose viscosity varies inversely with the rate of shear applied to the fluid. The Type II fluid is also called a thickened fluid, because it has the viscosity of a gel when sitting on the wings of a grounded airplane. But during takeoff, the air rushing over the wings exerts a shear stress on the fluid, thus reducing its viscosity and allowing the fluid to flow off the wing.

Prior to the IRT tests, the AEA and Boeing had conducted a joint flight test program on a Boeing 737 aircraft to evaluate the Type I and Type II fluids during take off. The results of those tests were as follows: During takeoff, as the airspeed over the wing increased, the fluid surface became wavy and the fluid began to run off the wing, but it also accumulated near the trailing edge. The waviness roughened the upper airfoil surface, and the fluid accumulation near the trailing edge decambered the airfoil. Both of these effects caused a loss in lift, an increase in drag, and a reduced stall angle-of-attack. The last effect was observed later in the wind tunnel tests, but not in the flight tests because the aircraft was not flown into stall while so close to the ground.

Tests were conducted on two models in the IRT: (1) a 0.091 scale 3D half model of the Boeing 737-200 ADV aircraft, and (2) a 0.18 scale 2D airfoil section at the 65 percent span of the 737-200 ADV aircraft (Fig. 31 and 32 respectively). Wind tunnel test objectives were as follows: (1) correlate wind tunnel and flight test measurements of aerodynamic effects of de-/anti-icing fluids; (2) evaluate fluid effects that could not be safely performed during flight tests; (3) expand flight test results for parametric variations of temperature, airfoil configuration, and fluid formulation; (4) contribute to the data base for establishing aerodynamic acceptance standards for ground de-/anti-icing fluids; and (5) obtain data that contributes to a physical understanding of the lift loss mechanism.

The data obtained from the wind tunnel tests included (1) model force data from internal balances; (2) surface static pressures; (3) initial fluid film depth from a gap gauge, (4) fluid film depth from a relationship between depth and photographed fluorescent intensity (a fluorescent dye added to the fluid and illuminated with ultra-violet light); (5) video recordings of fluid flow-off characteristics; and (6) boundary layer velocity profiles.

Typical results are shown in bar chart form in Fig. 33 where the percent loss in lift at 8° angle-of-attack and also at stall are presented for the Type I (labeled 1) and Type II (labeled 3) fluids and eight experimental Type II fluids. All of the experimental fluids showed lower lift loss than the then-current Type II fluid, and the losses for the experimental fluids were comparable to the losses for the Type I fluid.

An important outcome of this test program was that the experimental Type II fluids tested in the IRT in April 1988 have now become the current operational fluids in Europe. Another significant outcome is that these quantifiable test results showed that these new Type II fluids do not degrade takeoff aerodynamic performance anymore than do the Type I fluids. The Type II fluids have been shown by the AEA to have far greater holdover times than the AEA Type I fluids.

NASA also is funding research by Dr. C.S. Yih at the University of Florida to derive an analytical model of the surface instability that causes the fluid waves on the airfoil. Dr. Yih has identified the instability as being driven by the large fluid-to-air viscosity ratio. He has also derived dimensionless parameters that should be preserved during scale model testing to assure that model test results will represent full-scale results. A paper on the analytical formulation and mathematical solution will be published later.

DROPLET SIZING INSTRUMENTATION FOR ICING CLOUDS

Very accurate droplet size data is needed to validate droplet trajectory codes, such as the one used in LEWICE. And automated droplet sizing systems are needed to calibrate the IRT in a shorter time and with far fewer personnel than were employed in the earlier calibration program of the 1950's. NASA's droplet sizing effort is divided into two parts: (1) research to devise methods of calibrating and checking the accuracy of existing droplet sizing instruments; and (2) development of a new instrument that promises to overcome some of the known problems of the existing instruments.

Calibration Devices for Existing Wind Tunnel and Flight Instruments

Reference 33 presents a detailed review of the droplet sizing research conducted to understand the calibration and operation of two instruments manufactured by Particle Measuring Systems, Inc. (PMS): the FSSP (forward scattering spectrometer probe) and OAP (optical array probe).

A rotating pinhole device (Fig. 34) was developed (Refs. 33 and 34) to check the calibration of the FSSP. A calibration curve of the FSSP using rotating pinholes is given in Fig. 35. The value of this device is that it can be inserted into the FSSP probe volume at anytime to check whether the instrument is scattering light into the correct droplet size bin. This device can uncover misalignment of the laser or its optical system, it can measure optical parameters such as depth-of-field and optical collection angles, it can detect dirt or other contamination on the laser optics, and it can detect problems with the electronics systems. The device has proved invaluable in the recent calibration of the IRT, where it was demonstrated that such a calibration device is absolutely essential to the proper field operation of the FSSP.

NASA has checked the sizing accuracy of the FSSP by three methods: (1) pinholes, (2) glass beads, and (3) a water droplet generator. The results of these checks are shown in Fig. 36 where it can be seen that at the mid to upper range of the FSSP, the measured droplet size begins to depart significantly from the actual size. Thus in clouds with large droplets, the FSSP would undersize the median volume diameter 5 to 10 μm.

The Optical Array Probe (OAP) is used to measure droplets from 10 to 620 μm. NASA has developed a rotating reticle calibration disk for the OAP that provides absolute calibration over the entire size range of the OAP (Refs. 33 and 35). Figure 37 shows the calibration curve for the OAP using the rotating reticle.

When calibrating the icing cloud in the IRT, both the FSSP and the OAP were required because the droplet size range extended beyond the range of the

FSSP alone. Thus results from the OAP and FSSP had to be spliced together to obtain a continuous droplet distribution. Unfortunately, the splicing process is not exact, and since the median volume diameter (MVD) of the cloud is extremely sensitive to the number of larger droplets, the measurement of the larger MVD's has an indeterminate uncertainty.

Development of a Wind Tunnel and Flight Instrument

A newer instrument developed by Aerometrics, Inc., named the Phase Doppler Particle Analyzer (PDPA), shows promise of eliminating some of the limitations we have in calibrating the IRT with the FSSP and OAP (Ref. 36). NASA has worked very closely with Aerometrics to upgrade the laboratory PDPA instrument. These upgrades, which center on the signal processor, will result in the following improvements: (1) measurement of particles with velocities representative of flight speeds; (2) increase in dynamic size range from 35 to 50 (dynamic size range is the ratio of largest particle size to smallest particle size); and (3) greater size accuracy at high speeds and dense sprays. These upgrades, when completed, should allow us to use a single instrument for measuring the entire operating envelope of the IRT cloud.

Currently, the PDPA is a laboratory instrument that can probe clouds up to about 2 ft in depth. But in its present form, it cannot be used in the IRT, whose test section is 1.82 by 2.74 m (6 by 9 ft). Nor can it be used in an aircraft to sample clouds. To convert the laboratory PDPA for use on aircraft or the IRT, Aerometrics was awarded Phase I and Phase II Small Business Innovative Research contracts. For the flight version, a small transmitter and receiver unit will be placed in the cloud and the laser light will be sent to and from the unit by fiber optic cables. The Phase II contract is for 2 years and is just getting under way.

EXPERIMENTAL ICING FACILITIES

The NASA Icing Research Tunnel has for several years been one of NASA's most heavily scheduled wind tunnels, with tests scheduled up to two years in advance. In 1988, the tunnel logged 1330 test hours, which is the highest annual usage on record since 1950. The IRT is the largest refrigerated tunnel in the world. The test section is 1.82 m high by 2.74 m wide by 6.09 m long (6 ft high by 9 ft wide by 20 ft long). Its maximum airspeed empty is 134 m/sec (300 mph), and its maximum airspeed with a model installed depends on the model blockage. The IRT can provide tunnel total temperatures from 0 to -35 °C (+32 to -30 °F). Two different sets of nozzles are available for producing supercooled icing clouds that cover most, but not all, of the FAA Part 25 Appendix C icing envelopes.

Recent Rehabilitation of the NASA Icing Research Tunnel

Two years ago, the IRT underwent extensive renovations aimed at improving its reliability and productivity. The major improvements are as follows: (1) a new spray bar system, which has eight bars to provide a more uniform cloud than did the original six bars; (2) a new 3.73 MW (5000 hp) drive motor; (3) new solid state controls for the drive motor; (4) a new distributed process control system, which provides programmable, digital control of the drive

motor, the refrigeration system, the spray bar system, and other support systems; (5) a three-times-larger control room with vastly improved acoustics; (6) new electrical power supplies for operation of aircraft test models while in the IRT; and (7) replacement of all wooden floors with concrete floors.

Figure 38 shows a schematic of the IRT flow circuit and identifies the components that were rehabilitated. These improvements not only have increased productivity, but also have provided new test capabilities. For example, the Boeing/NASA ground deicing fluids test program, which required ramping the IRT airspeed to simulate takeoff, could not have been done with the old drive motor and controls.

Recalibration of the NASA Icing Research Tunnel

The purpose of the IRT is to simulate a flight through natural icing clouds. The quality of that simulation depends on its calibration for the following parameters: the aerothermodynamic variables of airspeed, temperature, and turbulence level; and the icing cloud variables of liquid water content and droplet size. Other simulation issues, such as scaling, are resolved by analyses and experimental technique.

The recent calibration included all of the above parameters. Figure 39 shows a preliminary droplet size calibration for the IRT "standard" nozzles. Figure 40 shows the IRT operating envelope for both the "standard" and "mod 1" nozzles at a tunnel airspeed of (112 m/sec) 250 mph. This was the first recalibration of the spray nozzles since 1956. One improvement over the old calibration is that the upper limit on calibrated MVD droplet size has been increased from 20 to 40 μm.

Tunnel Simulation Versus Natural In-Flight Tests

Flow turbulence level is always an element of concern in an icing tunnel because both the physical blockage of spray bars and the water and air that come out of the spray bars should affect turbulence. Since turbulence level in the IRT would affect both the ice accretion process and the evaluation of thermal ice protection systems, users often want to know about the IRT's turbulence level and if it adequately simulates inflight conditions.

The turbulence level in the IRT test section, as measured by VanFossen (Ref. 37) with hot wires, is about 0.5 percent when the water and air to the spray bars are turned off. Obviously, the turbulence level cannot be measured with the cloud on because the water droplets striking the hot wires would invalidate their readings. But we have tried to measure the turbulence level with the hot (180 °F) spray bar air turned on. At first it appeared that a valid hot wire reading was possible, but after careful study, VanFossen decided that filaments of the hot spray bar air may have been hitting the hot wires and giving incorrect readings.

To address the heat transfer question for the IRT, NASA measured heat transfer performance on a NACA 0012 airfoil (53.3 cm (21 in.) chord) in the IRT (with hot spray bar air turned on) and compared it with heat transfer performance on the same model in flight (Ref. 38). The model was extended out the overhead hatch of the Twin Otter as shown in Fig. 41. Figure 42 shows a

plot of Frossling number versus location on the airfoil for data taken in flight and in the IRT (Ref. 39). The figure shows that there is no distinguishable difference between heat transfer in flight and in the IRT.

FUNDAMENTAL STUDIES IN ICING

NASA maintains a strong effort in icing fundamentals, which is the backbone of any program that is developing new computer codes and new test techniques. We have already described several fundamental studies, for example, in formulating a new description of the ice accretion process, and in obtaining fundamental flowfield data for flow over ice shapes that cause flow separation and reattachment. In this section we review work on two important problems: icing scaling laws, and structural and adhesive properties of in-flight ice.

Icing Scaling Laws

The proposed or desired test matrix for an icing test usually involves the following variables: airspeed, outside air temperature, altitude, cloud liquid water content, cloud droplet size distribution or median volume diameter, and model size or scale. In a flight test in natural icing, or in an artificial cloud behind an in-flight spray tanker, chances are that the exact set of variables desired will be unattainable. In a wind tunnel test, certain combinations of variables also will be unattainable. For example, most icing wind tunnels have maximum airspeeds far below the speeds of modern transport or military aircraft. And due to the practical limits on nozzle turn-down ratios and nozzle droplet size ranges no wind tunnel can achieve the full FAA Part 25 Appendix C operating envelopes over the full speed range of the tunnel.

If the desired test variables cannot be met, the experimenter must resort to some form of scaling. Various objectives can be imagined for any particular scaled test: (1) a geometrically similar ice shape; (2) an equivalent drag coefficient for the ice shape/model combination; (3) the same water flux around the airfoil leading edge; (4) the same heat transfer results for a thermal ice protection system; (5) rime icing conditions (i.e., all water must freeze immediately upon impact); and so on. Scaling laws have always been used, but never rigorously validated (Ref. 40). This does not mean the tests were done incorrectly, for icing has been and always will be part science and part art. This is why inflight testing in natural icing clouds always will be a required part of the certification/qualification process.

Reference 40 gives a good bibliography of the work done previously on scaling. Most of these works on scaling rely on an analysis of the ice accretion process described by Messinger (Ref. 13) over 30 years ago. New insights into the ice accretion process by Olsen (Ref. 14) and Hansman (Refs. 15 and 16) have led Bilanin (Ref. 41) to apply the Buckingham pi theory to the ice accretion problem. Bilanin showed that the normalized thickness of the ice accreted on the airfoil is a function of 18 nondimensional groups. Although many of the groups are satisfied in any scaling test, there exists a problem holding Mach, Reynolds and Weber numbers constant between tests. He concluded that the old Messinger formulation may be inadequate, and that improved ice accretion scaling may require a better match in Reynolds number and consideration of the physics of water film and droplet splash dynamics on the airfoil surface.

In Ref. 41 Bilanin concluded that competing physical effects do not in general allow a rigorous scaling methodology, but an acceptable approximate scaling scheme may be possible. He has suggested a series of tests on rotating and nonrotating cylinders to validate the approximate schemes. NASA plans to participate in a joint Air Force/FAA/NASA program to carry out these suggested tests later this year.

Structural and Adhesive Properties of In-Flight Ice

Over the past 5 years, NASA has supported a continuous, but low-level effort to study the structural properties of ice formed in flight. This work is described in Refs. 42 to 47. Ice formed in flight or in an icing research tunnel results from supercooled water droplets impacting a surface at flight speed or wind tunnel airspeed. We refer to ice so formed as 'impact' ice. Impact ice can vary in type over a wide range, depending on the liquid water content and droplet size distribution in the cloud, on the outside air temperature, and on the droplet velocities. The adhesion of ice to a surface depends not only on the type of ice formed, but also on the roughness, porosity, and other fundamental properties of the surface. The statistical variation of ice properties from one test to the next is a real phenomenon, and it must be accounted for in the design of systems that depend on ice shedding for their operation.

The overall objectives of the project are (1) to measure the structural properties of impact ice, such as, basic tensile properties, adhesive characteristics, and peel properties and (2) to develop finite element analytical methods for use in the analysis and design of deicing systems and icing testing apparatus.

Test apparatuses have been designed to measure each of the three basic mechanical properties: (1) tensile (Young's modulus (E), and ultimate tensile strength of impact ice in a direction transverse to the direction of ice growth); (2) shear (adhesion); and (3) peeling. Data has been obtained on both adhesive shear strength of impact ices and peeling forces for various icing conditions. Being studied are the influences of key parameters, such as, tunnel temperature, wind velocity, water drop size, substrate material, substrate surface temperature, and ice thickness. A finite element analysis of the shear test apparatus was developed in order to gain more insight into the evaluation of the test data.

Measurements indicate that surface roughness has a major effect on the adhesive shear strength. Additional adhesive shear strength tests are planned in which the surface roughness will be systematically varied.

Fixed airfoils, rotor blades, and propellers are being studied. In these studies, the adhesive shear strength of the impact ice is an important parameter. Surface roughness and the statistical nature of the data must be considered. For rotating surfaces, not only is the adhesive strength important but also the tensile strength of the ice perpendicular to the direction of growth. At the present time, the finite element analysis of rotating airfoils is being emphasized. Analytical results will be compared to recent data from the OH-58 tail rotor tests in the IRT. The statistical nature of the fracture of impact ice will be considered in the analysis.

The NASTRAN finite element code was also used to predict deicing of an EIDI ice protection system, for which experimental data was available (Ref. 46). Even though additional correlations with other data are needed, results from this initial study were encouraging.

There is a possibility that a fracture mechanics approach could be used to predict the pealing of ice from deicing systems such as a pneumatic boot. Data obtained from pealing measurements is being reduced to obtain the critical stress intensity constant of fracture mechanics.

REFERENCES

1. Reinmann, J.J., Shaw, R.J., and Olsen. W.A.; "Aircraft Icing Research at NASA," June 1982, NASA TM-82919.

2. Shaw, R J ; "Progress Toward the Development of an Aicraft Icing Analysis Capability," Jan. 1984, AIAA Paper 0105.

3. Shaw, R.J., Potapczuk, M.G., and Bidwell, C.S.; "Predictions of Airfoil Aerodynamic Performance Degradation Due to Icing," Fourth Symposium on Numerical and Physical Aspects of Aerodynamic Flows, Jan. 1989.

4. Ranaudo, R.J., Reehorst A.L., and Potapczuk, M.G., "An Overview of the Current NASA Program on Aircraft Icing Research," Oct. 1988, SAE Technical Paper 881386.

5. Keith, T.G., DeWitt, K.J., Wright, W.B., and Masiulaniec, K.C., "Overview of Numerical Codes Developed for Predicted Electrothermal De-Icing of Aicraft Blades," Jan. 1988, AIAA Paper 88-0288.

6. Goldberg, J., and Lardiere, B., "Developments in Expulsive Separation Ice Protection Blankets," Jan. 1989, AIAA paper 89-0774.

7. Zumwalt, G.W., Schrag, R.L., Bernhart, W.D., and Friedberg, R.A., "Electro-Impulse De-Icing Testing Analysis and Design," 1988, NASA CR-4175.

8. Zieve. P.S.: private communication.

9. Berkowitz, B.M., and Riley, J.T , "Analytical Ice Shape Predictions for Flight in Natural Icing Conditions," 1988, NASA CR-182234.

10. Olsen, W.A., Shaw, R.J., and Newton, J., "Ice Shapes and the Resulting Drag Increase for a NACA 0012 Airfoil," Jan. 1984, NASA TM-83556.

11. Van Fossen, G.J., Semonian, R.J., Olsen, W.A., and Shaw, R.J., "Heat Transfer Distributions Around Nominal Ice Accretion Shapes Formed on a Cylinder in the NASA Lewis Icing Research Tunnel," Jan. 1984, AIAA Paper 84-0017.

12. Scott, J.N., Gielda, T.P., and Hankey, W.L., "Navier-Stokes Solutions of Flowfield Characteristics Produced by Ice Accretion," Jan. 1988, AIAA Paper 88-0290.

13. Messinger, B.L.; "Equilibrium Temperature of an Unheated Icing Surface as a Function of Airspeed," Journal of Aeronautics Sciences, Jan. 1958.

14. Olsen, W., and Walker, E., "Experimental Evidence for Modifying the Current Physical Model for Ice Accretion on Aircraft Surfaces," May 1986, NASA TM-87184,

15. Hansman, R.J., and Turnock, S.R., "Investigation of Microphysical Factors Which Influence Surface Roughness During Glaze Ice Accretion," Fourth International Conference on Atmospheric Icing of Structures, Sept. 1988.

16. Hansman, R.I., Yamaguchi, K., Berkowitz, B., and Potapczuk, M., "Modeling of Surface Roughness Effects on Glaze Ice Accretion," Jan. 1989, AIAA Paper 89-0734.

17. Pulliam, T.H., "Euler and Thin-Layer Navier-Stokes Codes: ARC3D, ARC3D," Notes for Computational Fluid Dynamics User's Workshop, The University of Tennessee Space Institute, Tullahoma, TN, 1984.

18. Cebei, T., "Effects of Environmentally Imposed Roughness on Airfoil Performance," June 1987, NASA CR-179639.

19. Cebeci, T., Jau, J., Vitiello, D., and Chang, K.C., "Prediction of Post-Stall Flows on Airfoils," Fourth Symposium on Numerical and Physical Aspects of Aerodynamic Flows, Jan. 1989.

20. Potapczuk, M.G., "Personal Communication on Doctoral Dissertation. NASA Lewis Research Center, Cleveland, OH.

21. Bragg, M.B., and Khodadoust, A., "Effect of Simulated Glaze Ice on a Rectangular Wing," Jan. 1989, AIAA Paper 89-0750.

22. Sankar, L., Chiwu, J., and Huff, D., "Evaluation of Three Turbulence Models for the Prediction of Steady and Unsteady Airflows," Jan. 1989, AIAA Paper 89-0609.

23. Mikkelsen, K.L., McKnight, R.C., Ranaudo, R.J., and Perkins, P.J., Jr., "Icing Flight Research: Aerodynamic Effects of Ice and Ice Shape Documentation With Stero Photography," Jan. 1985, AIAA Paper 85-0468

24. Mikkelsen, K., Juhasz, N., Ranaudo, R., and McKnight, R., "In-Flight Measurements of Wing Ice Shapes and Wing Section Drag Increases Caused by Natural Icing Conditions," Apr. 1986, NASA TM-87307.

25. Ranaudo, R.J., Mikkelsen, K.L., McKnight, R.C., Ide, R.F., and Reehorst, A.L., "The Measurement of Aircraft Performance and Stability and Control After Flight Through Natural Icing Conditions," Apr. 1986, AIAA Paper 86-9758.

26. Ide, R.F., and Richter, G.P., "Comparison of Icing Cloud Instruments for 1982-1983 Icing Season Flight Program," Jan. 1984, NASA TM-83569.

27. Ranaudo, R.J., Mikkelsen, K.L., McKnight, R.C., and Perkins, P.J., Jr., "Performance Degradation of a Typical Twin Engine Commuter Type Aircraft in Measured Natural Icing Conditions," 1984, NASA TM-83564.

28. Ranaudo, R.J., Batterson, J.G., Reehorst, A.L., Bond, T.H., and Omara, T.M., "Determination of Longitudinal Aerodynamic Derivatives Using Flight Data From an Icing Research Aircraft," Jan. 1989, AIAA Paper 89-0754.

29. Batterson, J.G., and O'Mara, T.M. "Estimation of Longitudinal Stability and Control Derivatives for an Icing Research Aircraft From Flight Data," Mar. 1989, NASA TM-4099.

30. Miller, T.L., and Bond, T.H., "An Icing Research Tunnel Test of a Model Helicopter. To be presented at the American Helicopter Society 45th Annual Forum and Technology Display, Boston, MA, May 22-24, 1989.

31. Pike, J.A., Wainauski, H.S., and Boyd, L.S., "Prop-Fan Airfoil Icing Characteristics," Jan. 1989, AIAA Paper 89-0753.

32. Hill, E.G., Zierton, T.A., and Runyan, J.J., "Results of a Flight and Wind Tunnel Investigation of Aerodynamic Effects of Aircraft Ground De-/anti-Icing Fluids," Effect of an Adverse Environment on Flight, (AGARD Flight Mechanics Panel Symposium), Gol, Norway, May 1989.

33. Hovanec, E.A.; "Droplet Sizing Instrumentation Used for Icing Research: Operation, Calibration, and Accuracy; Phase I Final Report," NASA CR- (to be published jointly by NASA and FAA).

34. Hovenac, E.A., and Ide, R.F., "Performance of the Forward Scattering Spectrometer Probe in NASA's Icing Research Tunnel," Jan. 1989, AIAA Paper 89-0769.

35. Hovenac, E.A., Hirleman, E.D., and Ide, R.F., "Calibration and Sample Volume Characterization of PMS Optical Array Probes," International Conference on Liquid Atomization and Spray Systems, July 1985.

36. Bachalo, W.D., and Houser, J.J., "Phase Doppler Spray Analyzer for the Simultaneous Measurements of Droplet Size and Velocity Distributions," 1984, Optical Engineering, Vol. 23, no. 5, pp. 583-590.

37. VanFossen, G.J., "Private Communication. NASA Lewis Research Center, Cleveland, OH.

38. Newton, J.E., VanFossen, G.J., Poinsatte, P.E., and deWitt, K.J., "Measurement of Local Convective Heat Transfer Coefficients From a Smooth and Roughened NACA-0012 Airfoil Flight Test Data," Jan. 1988, AIAA Paper 88-0287.

39. Van Fossen, G.J.: Private Communication. NASA Lewis Research Center, Cleveland, OH.

40. Bilanin, A.J., "Proposed Modifications to Ice Accretion/Icing Scaling Theory," Jan. 1988, AIAA Paper 88-0203.

41. Bilanin, A.J., "Problems in Understanding Aircraft Icing Dynamics," Jan. 1988, AIAA Paper 89-0735.

42. Chu, M., Scavuzzo, R.J., and Olsen, W., "Measurement of Adhesive Shear Strength of Impact Ice in an Icing Wind Tunnel," Proceedings of 3rd International Workshop on the Atmospheric Icing of Structures, May 1986.

43. Scavuzzo, R.J., Chu, J.L., and Lam, P.D., "Development of a Composite Technique in the Determination of the Tensile Strength of Impact Ices. Proceedings of 3rd International Workshop on the Atmospheric Icing of Structures, May 1986.

44. Scavuzzo, R.J., Chu, M.L., and Olsen, W.A., "Structural Properties of Impact Ices Accreted at Aircraft Structures," Jan. 1987, NASA CR 179580.

45. Khatkhate, A.A., Scavuzzo, R.J., and Chu, M., "A Finite Element Study of the EIDI System," Jan. 1988, AIAA Paper 88-0022.

46. Chu, M., Scavuzzo, R.J., and Zian, X.T., "Hybrid Finite Element-Experimental Technique for Determination of Ice/Impact Ice Tensile Strength," Proceedings of the 4th International Conference on Atmospheric Icing of Structures, 1988.

47. Scavuzzo, R.J., Chu, M.L., and Brikmanis, C.K., "Adhesive Peel Strength of Artificial Ice," Proceedings of the 4th International Conference on Atmospheric Icing of Structures, 1988.

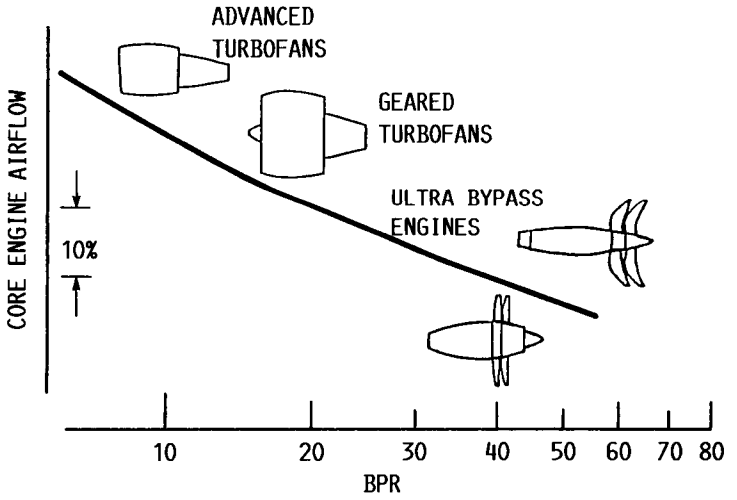

FIGURE 1. - ENGINE PERFORMANCE TRENDS; CORE ENGINE AIRFLOW VERSUS BY-PASS RATIO.

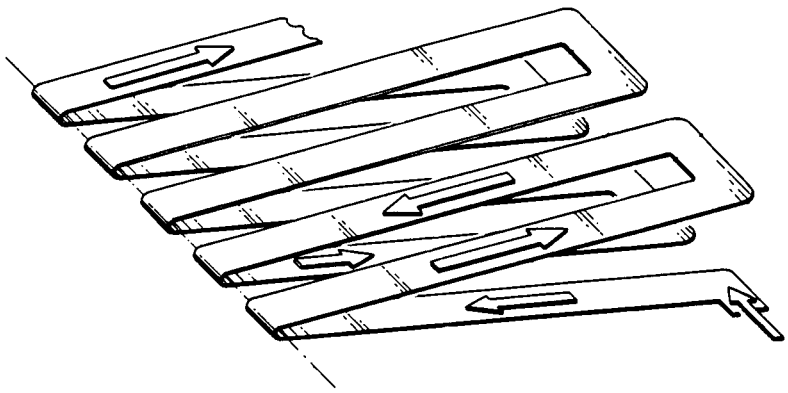

FIGURE 2. - EESS CONDUCTOR GEOMETRY.

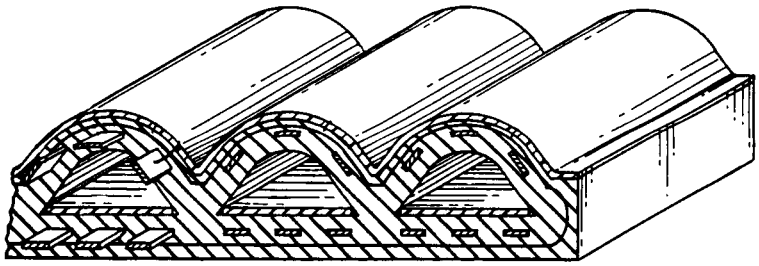

FIGURE 3. - EESS CONDUCTORS EMBEDDED IN ELASTOMERIC BOOT.

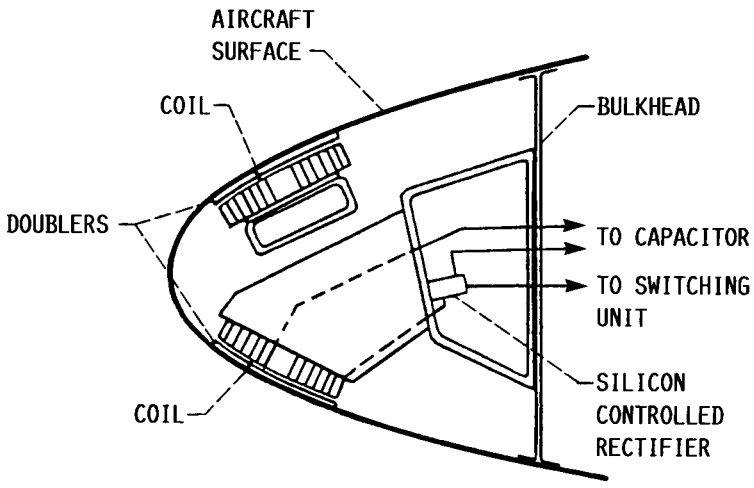

FIGURE 4. - EIDI COILS IN LEADING EDGE.

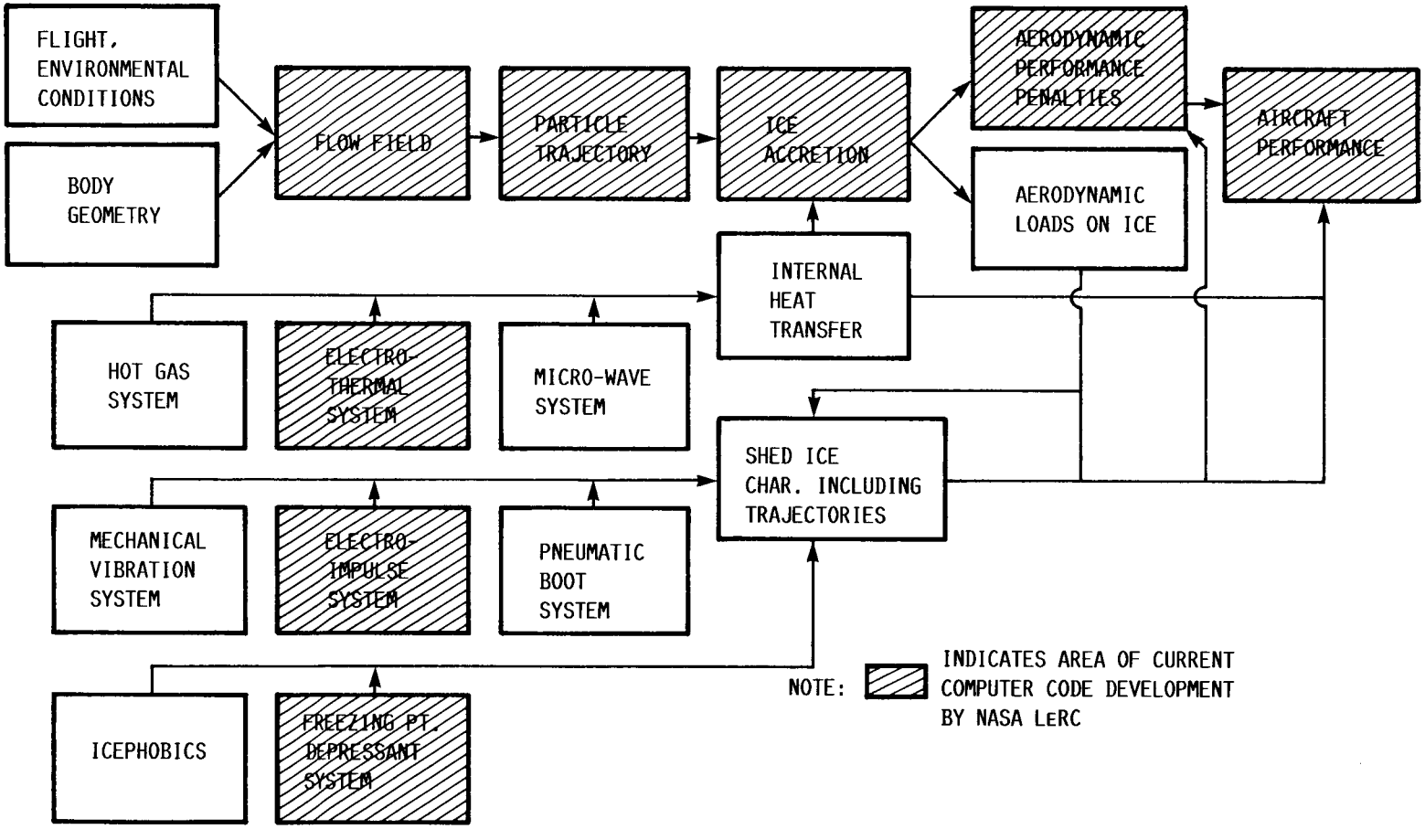

FIGURE 5. - AIRCRAFT ICING ANALYSIS METHODOLOGY.

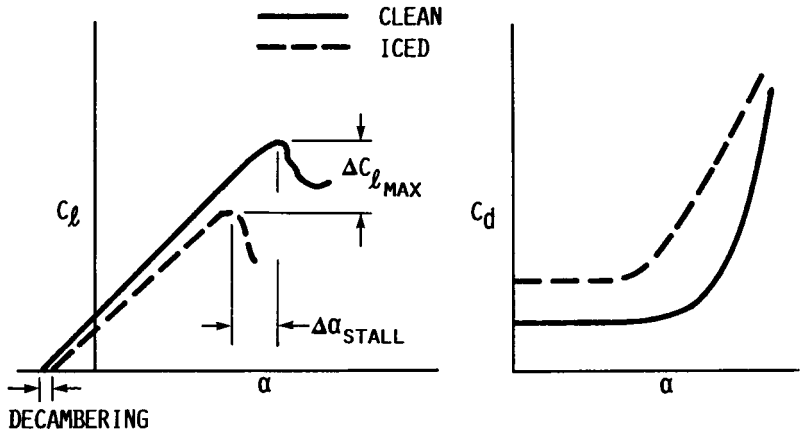

FIGURE 6. - AERODYNAMIC PERFORMANCE DEGRADATION DUE TO ICING.

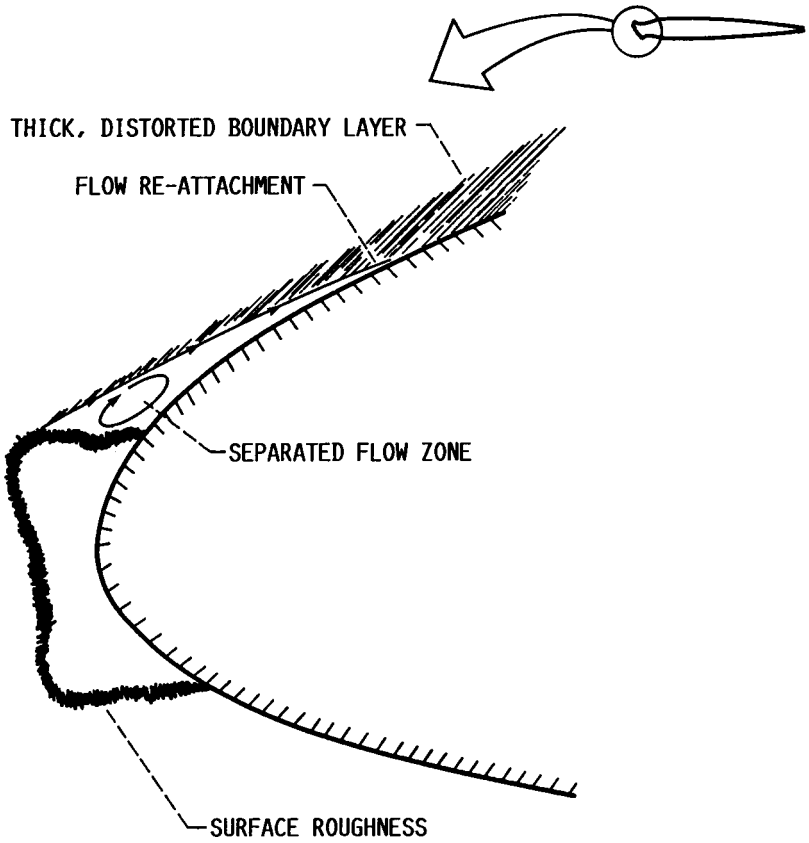

FIGURE 7. - KEY ASPECTS OF AIRFOIL ICING.

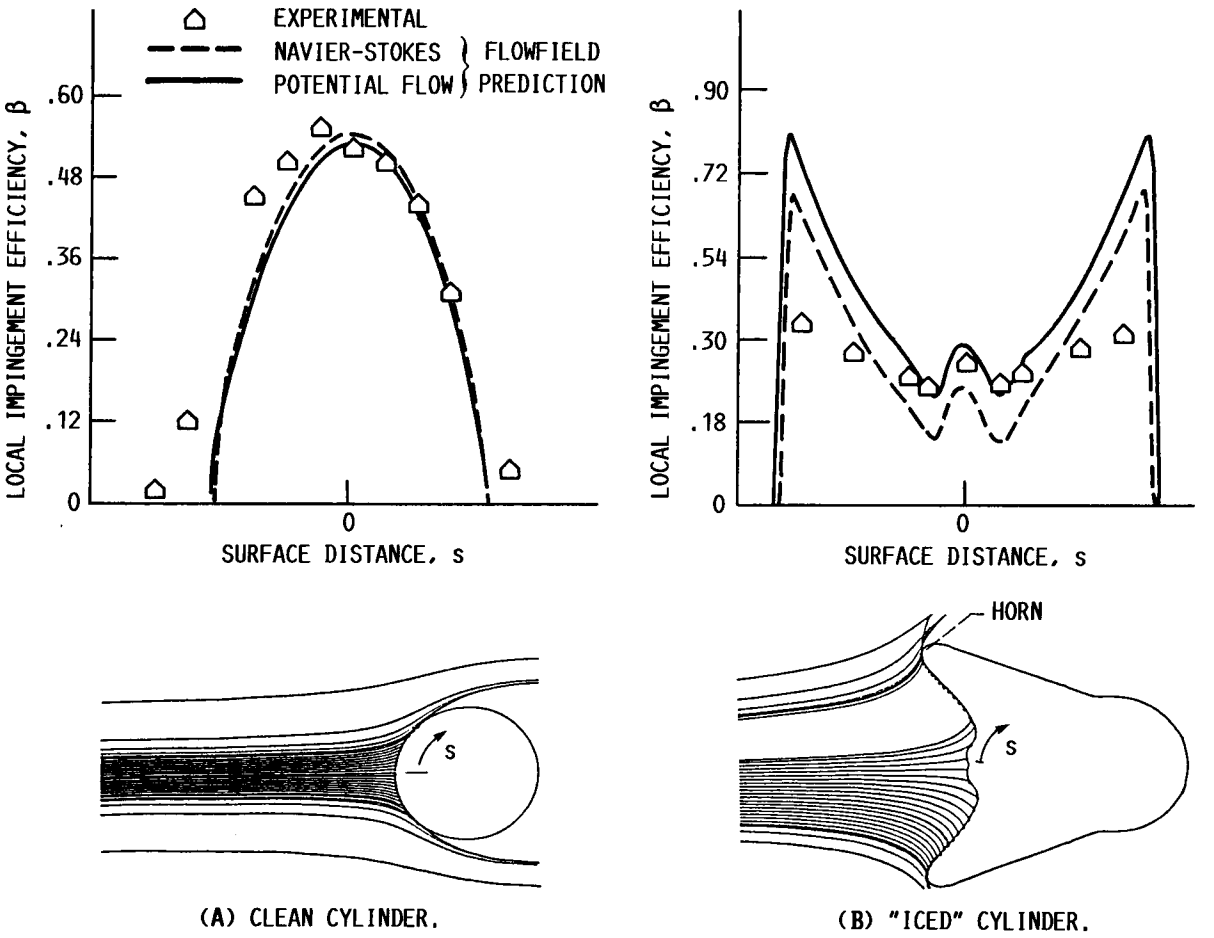

(A) CLEAN CYLINDER. (B) "ICED" CYLINDER.

FIGURE 8. - DROPLET COLLECTION EFFICIENCY COMPARISONS.

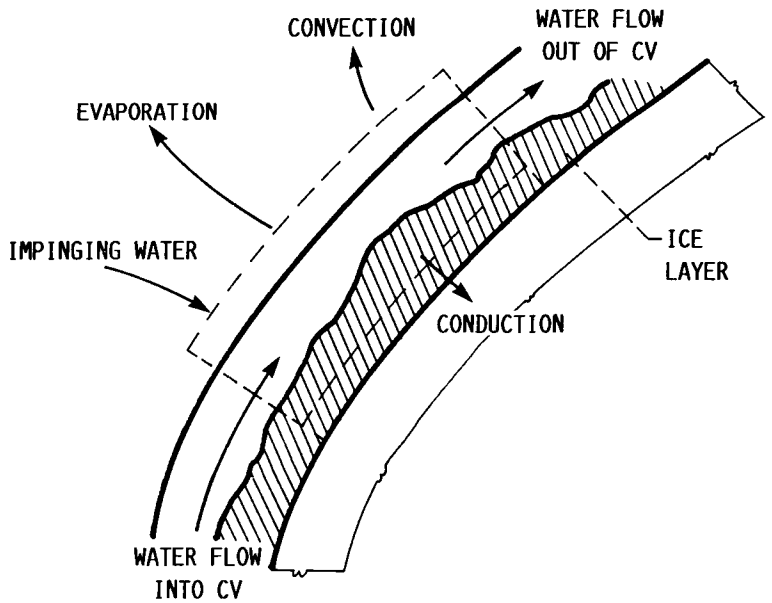

FIGURE 9. - CONTROL VOLUME ANALYSIS OF ICE ACCRETION PROCESS.

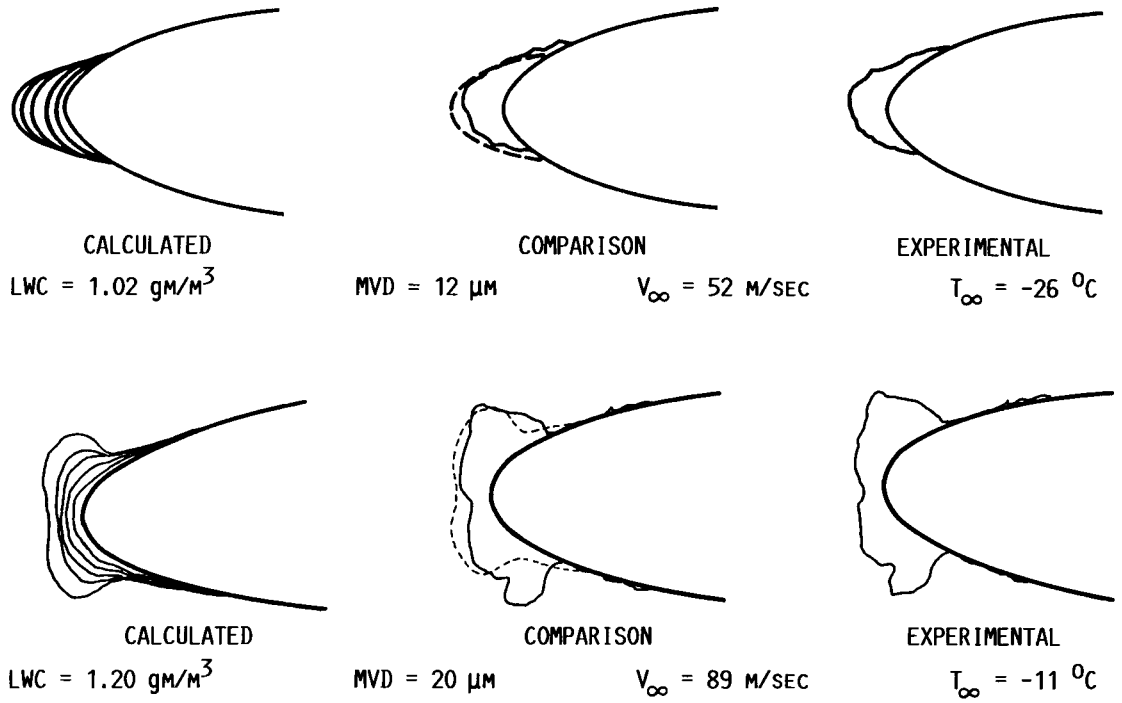

FIGURE 10. - COMPARISON OF ICE SHAPE PREDICTIONS WITH AIRFOIL ICING DATA.

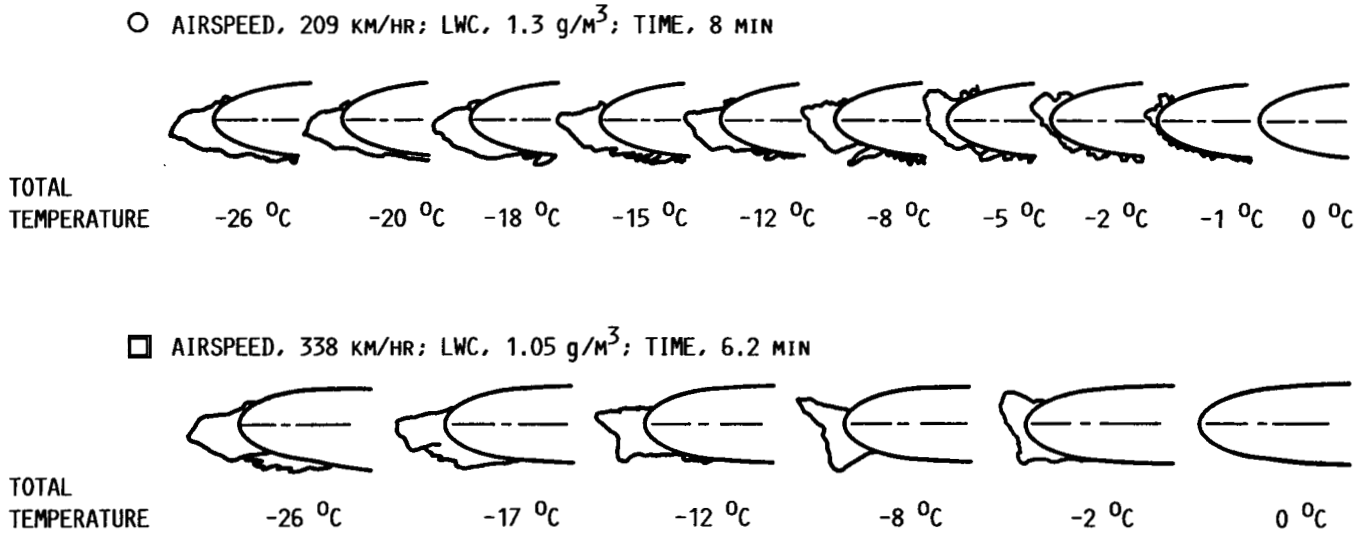

(A) ICE SHAPE.

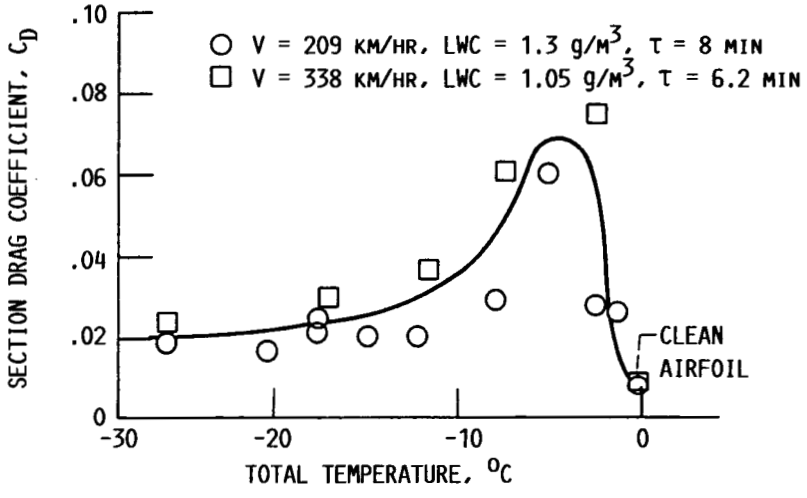

(B) SECTION DRAG COEFFICIENT

FIGURE 11. - EFFECT OF TOTAL TEMPERATURE ON ICE SHAPE AND DRAG.

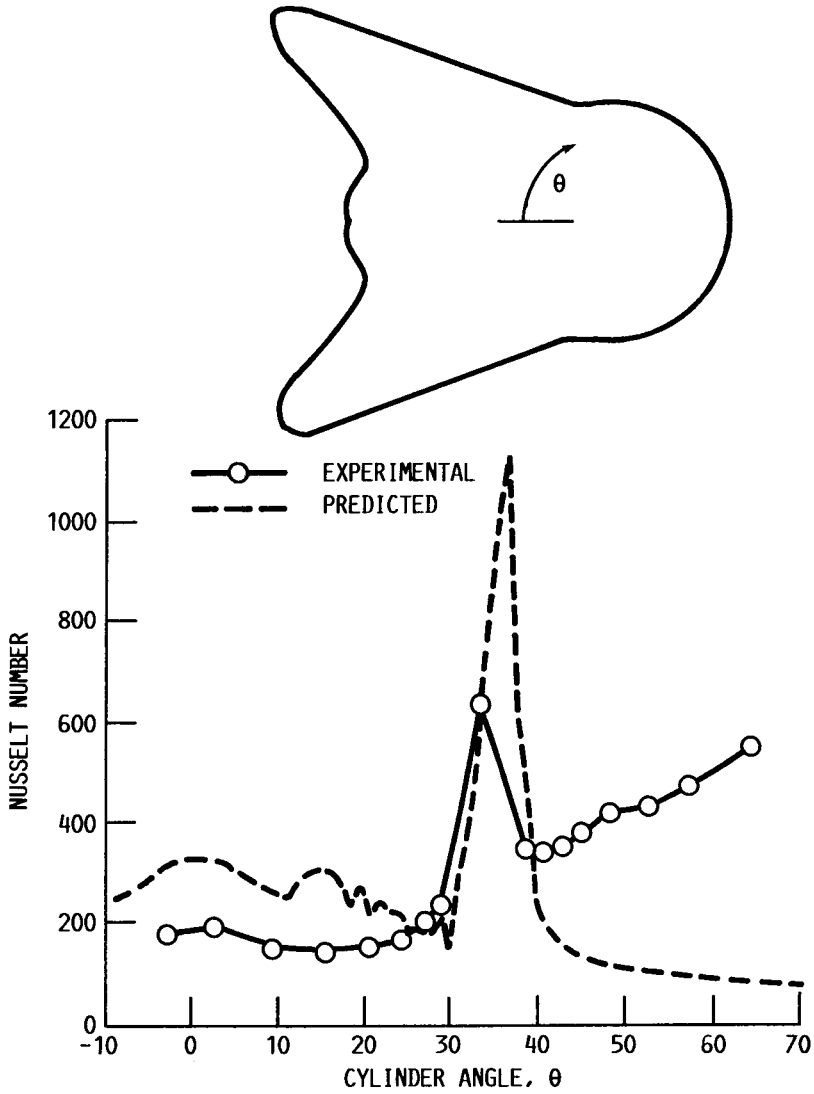

FIGURE 12. - NUSSELT NUMBER PREDICTION BASED ON INTEGRAL BOUNDARY LAYER METHOD.

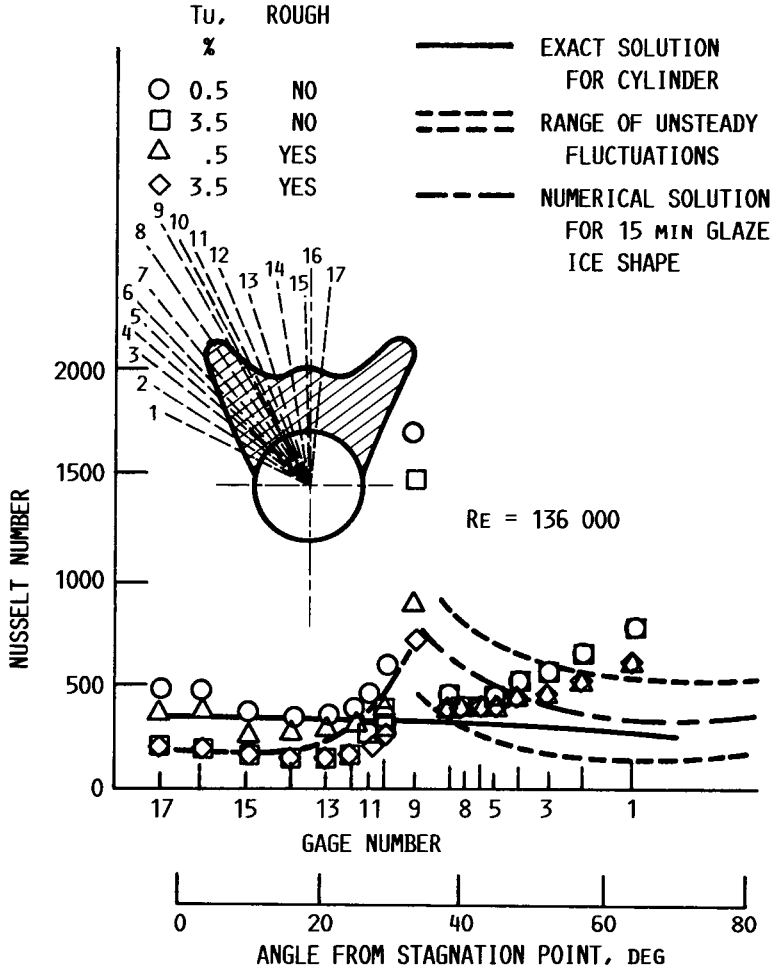

FIGURE 13. - NUSSELT NUMBER PREDICTION BASED ON NAVIER-STOKES SOLUTION OF ENERGY EQUATION.

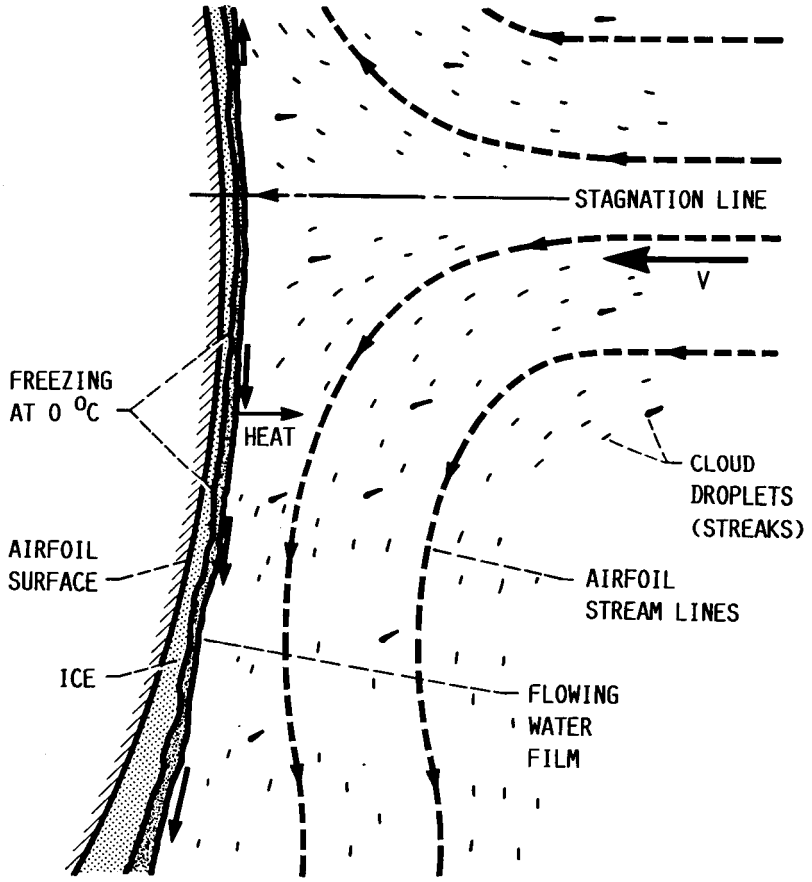

FIGURE 14. - EXISTING PHYSICAL MODEL FOR ICE ACCRETION.

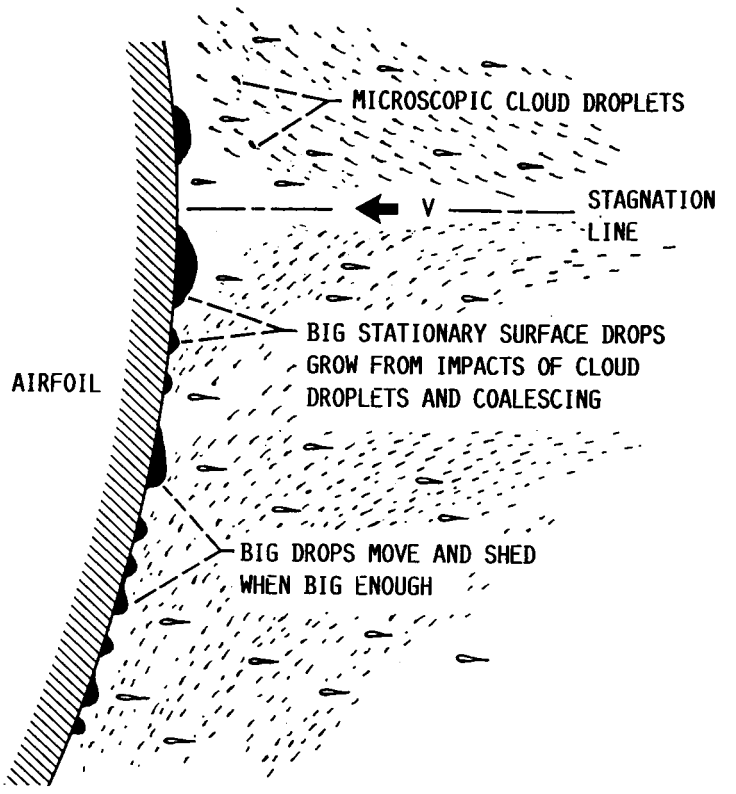

(A) NO FREEZING OCCURRING (ABOVE 0 ^{o}C OR BEFORE FREEZING STOPS SURFACE DROPS).

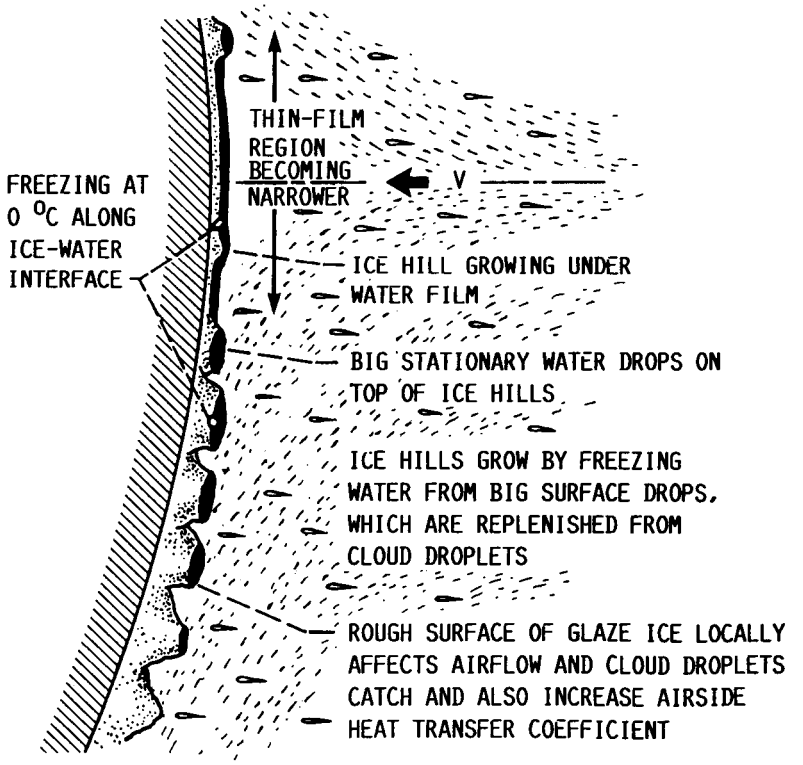

(B) FREEZING OCCURRING.

FIGURE 15. - PROPOSED NEW PHYSICAL MODEL FOR ICING PROCESS.

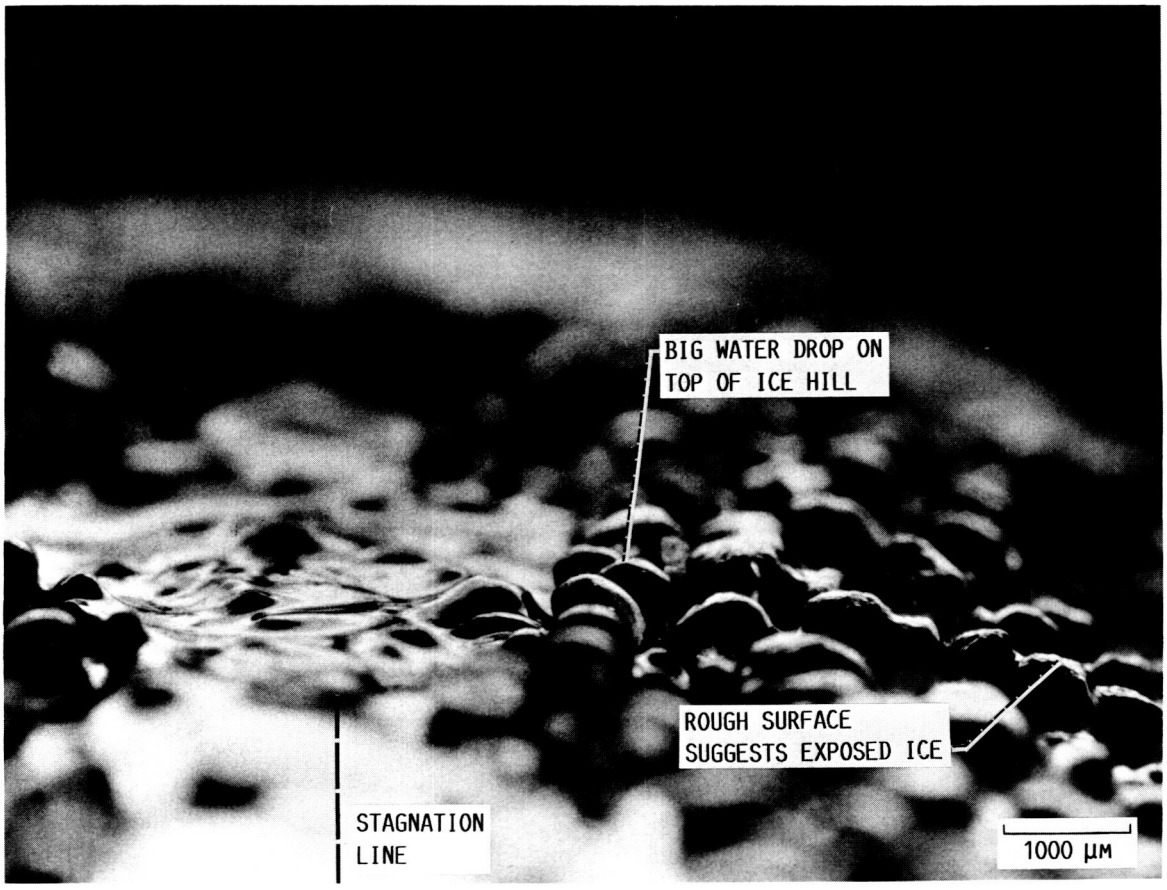

τ = 50 SEC

FIGURE 16. - CLOSE-UP PHOTO OF ICE FORMED AT -2 ^{o}C.

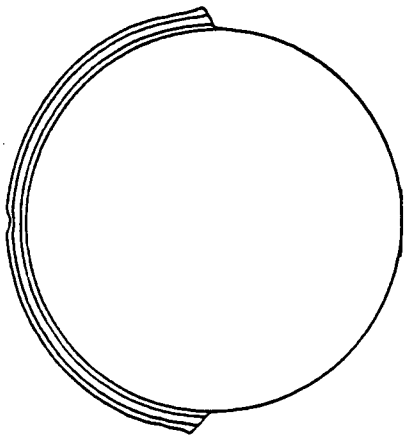

(A) NORMAL LEWICE AT 45, 105, AND 150 SEC.

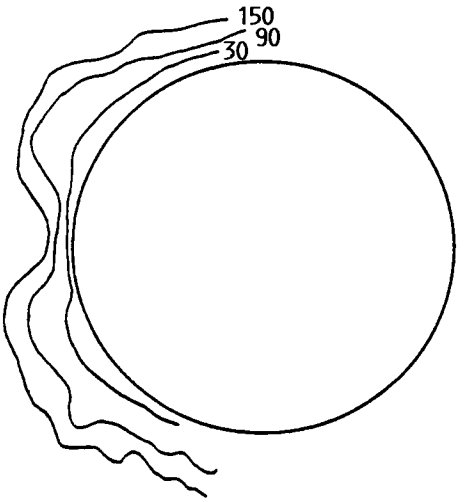

(B) EXPERIMENTAL RESULT AT 30, 90, AND 150 SEC.

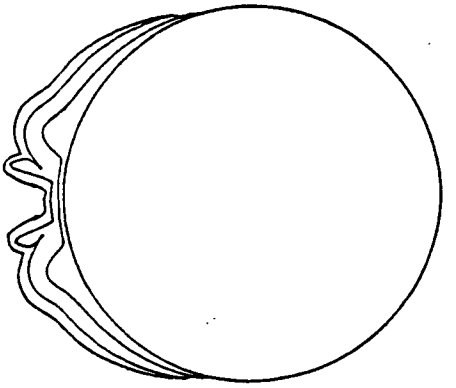

(C) MODIFIED LEWICE AT 45, 105, AND 150 SEC.

FIGURE 17. - EXPERIMENTAL ICE SHAPE COMPARED TO MODIFIED LEWICE PREDICTIONS.

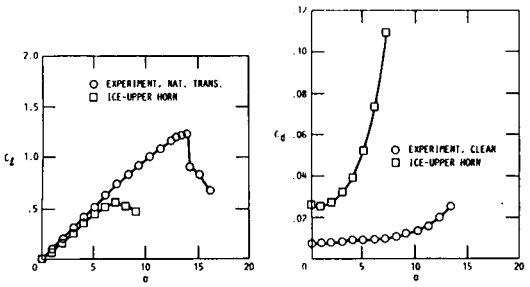

FORCE AND MOMENT DATA

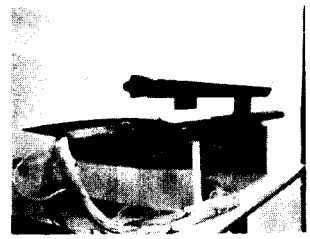

NACA 0012 MODEL

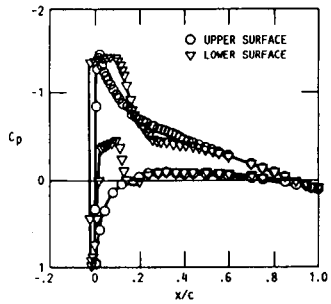

DETAILED SURFACE PRESSURES

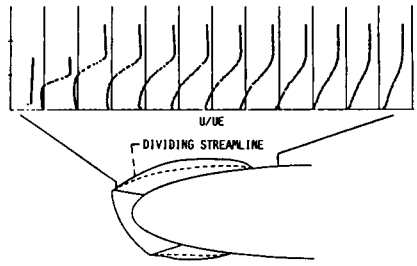

BOUNDARY LAYER PROFILES

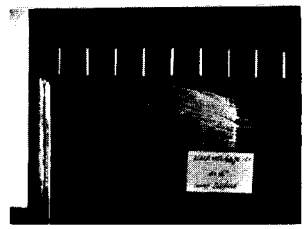

FLOW VISUALIZATION

LIFT COEFFICIENT

FIGURE 18. - CODE VALIDATION DATA BASE FOR ICED AIRFOIL PERFORMANCE.

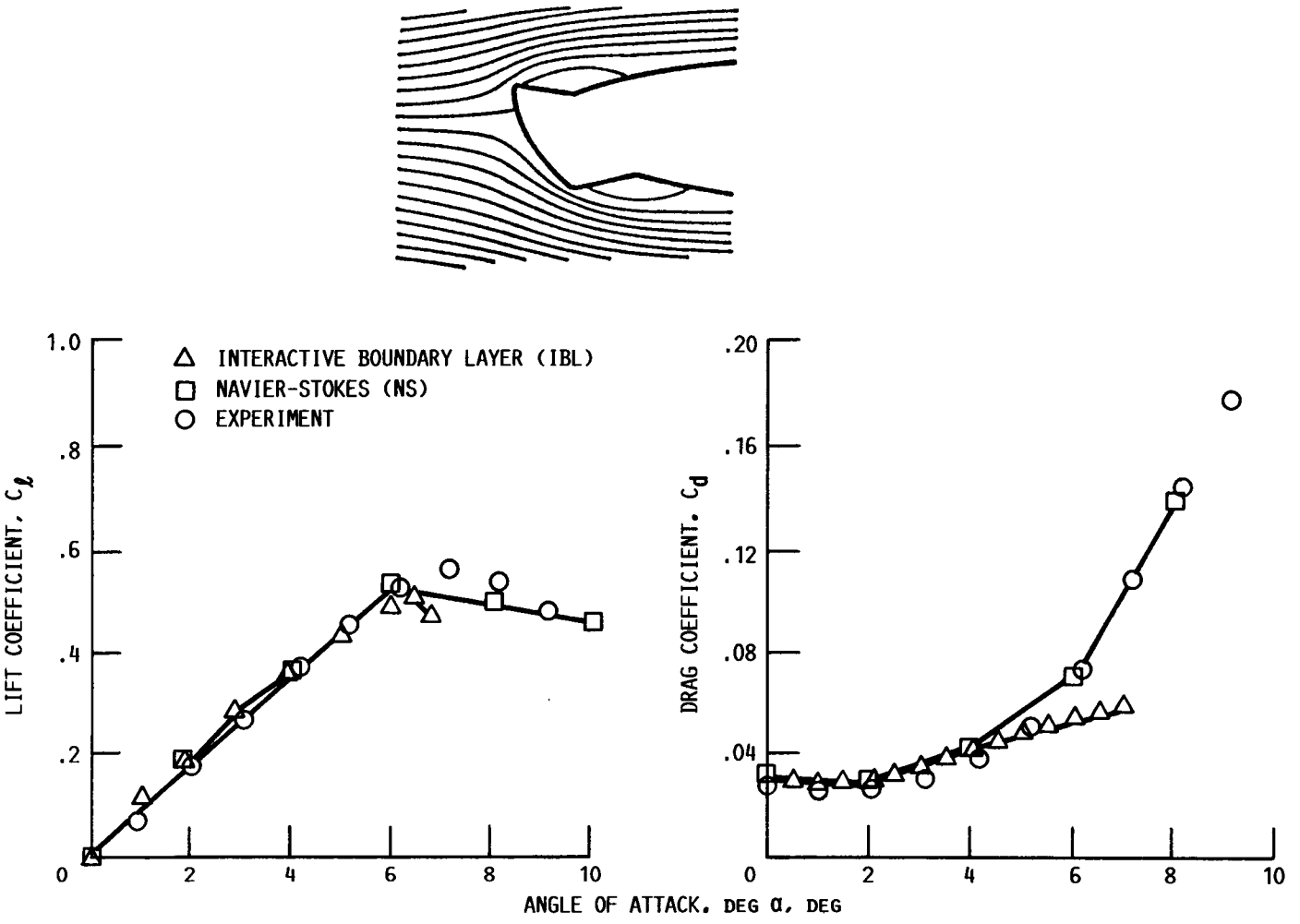

FIGURE 19. - COMPARISON OF CODE PREDICTIONS WITH EXPERIMENT FOR AN ICED AIRFOIL.

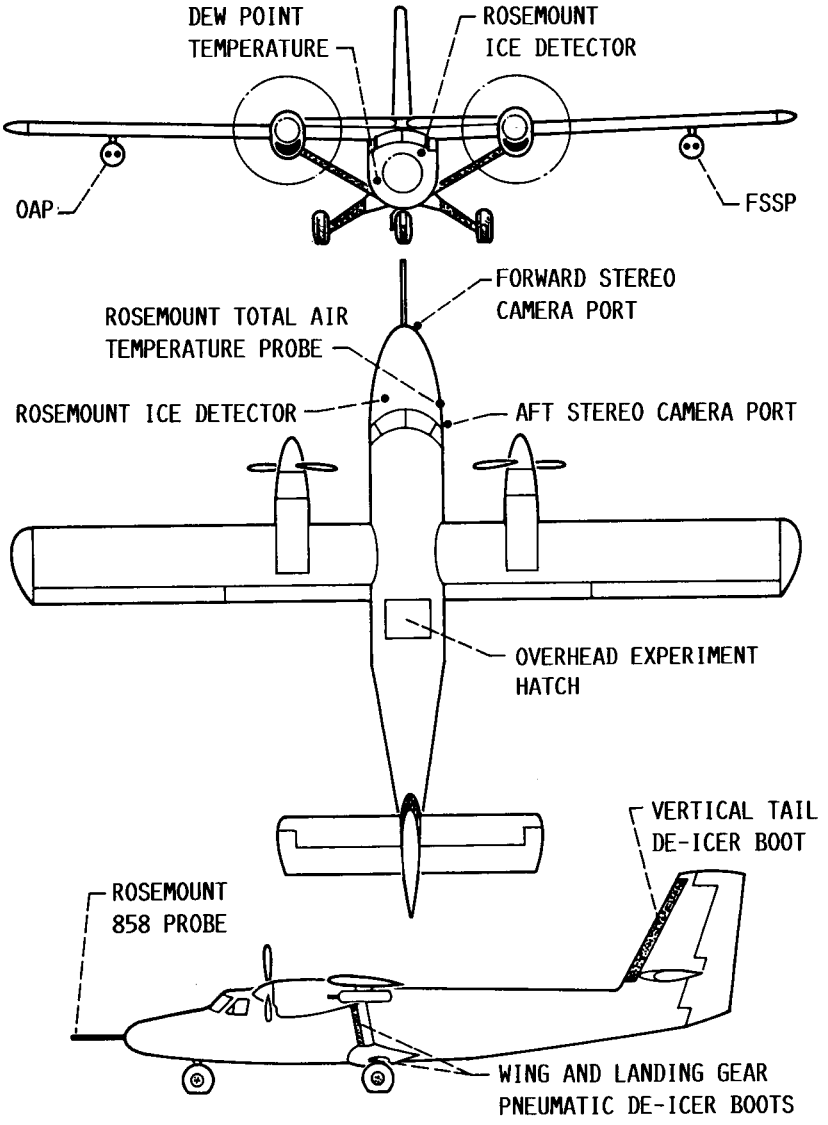

FIGURE 20. - NASA TWIN OTTER ICING RESEARCH AIRCRAFT.

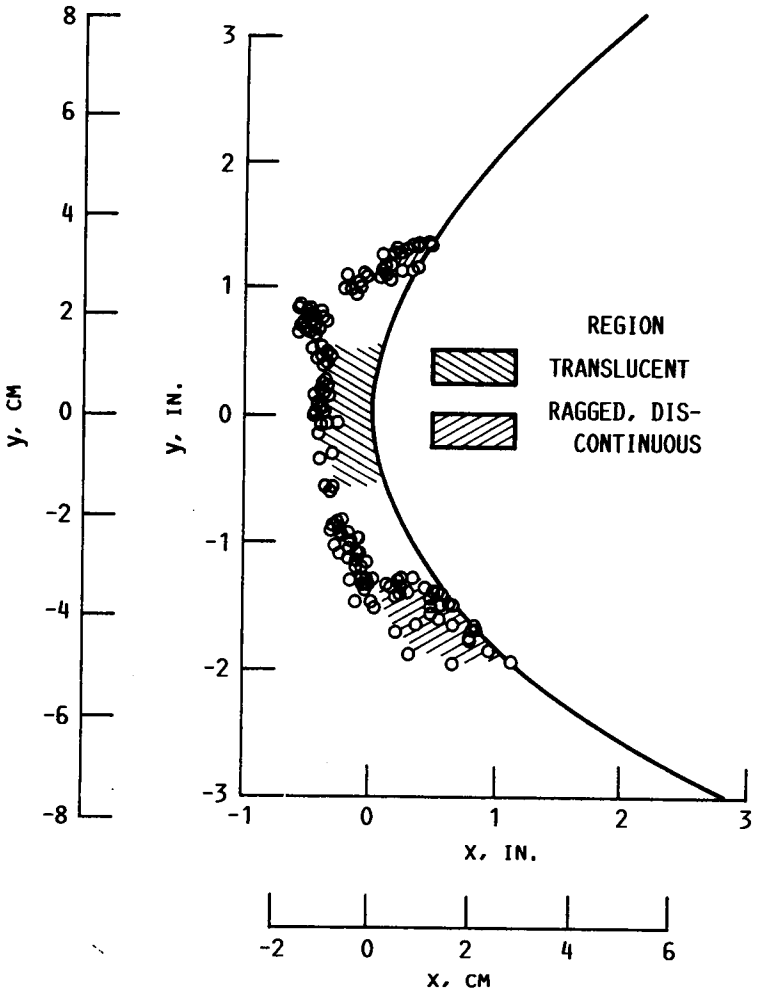

FIGURE 21. - ICE SHAPE PROFILE MEASURED BY STEREO PHOTOGRAPHY; FLIGHT 85-24B.

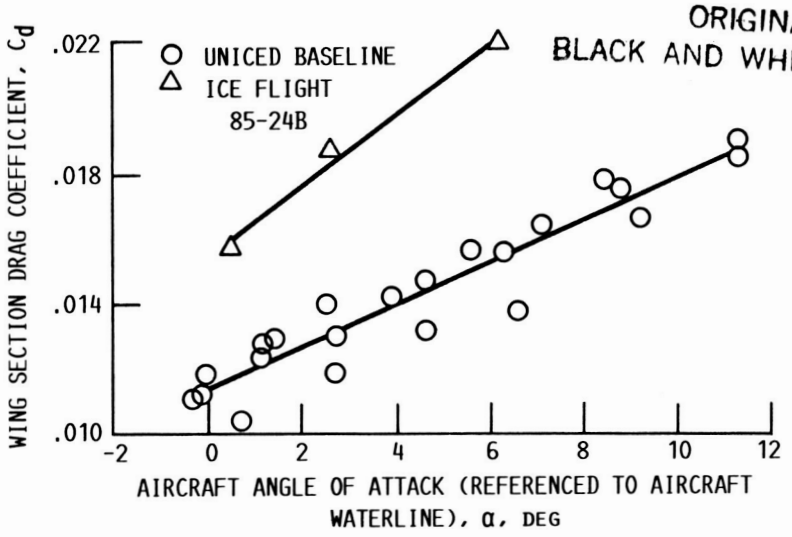

FIGURE 22. - INCREASE IN WING SECTION DRAG DUE TO ICE ACCRETION; FLIGHT 85-24B.

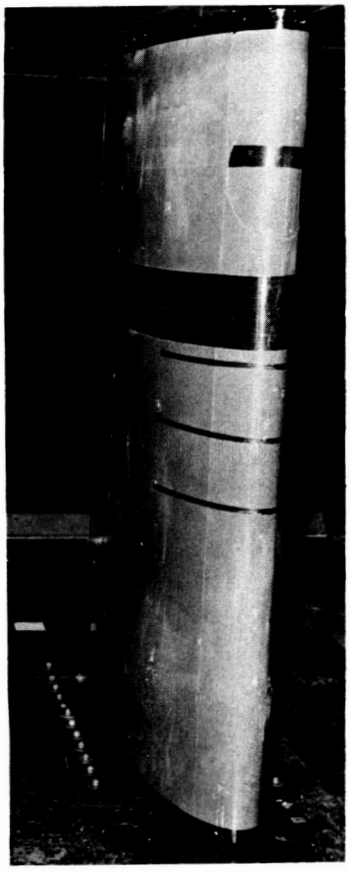

FULL SCALE WING SECTION IN IRT

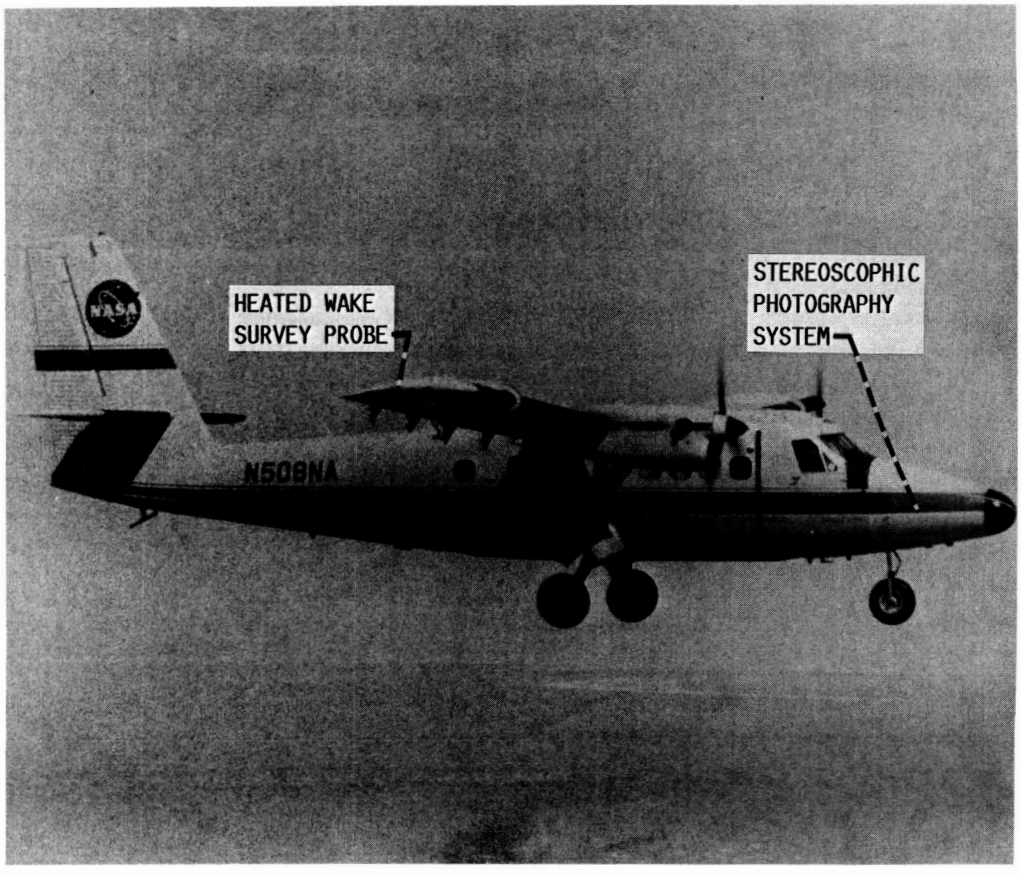

NASA ICING RESEARCH AIRCRAFT

FIGURE 23. - FLIGHT VERSUS TUNNEL COMPARISON OF AIRFOIL ICE ACCRETION AND DRAG INCREASE.

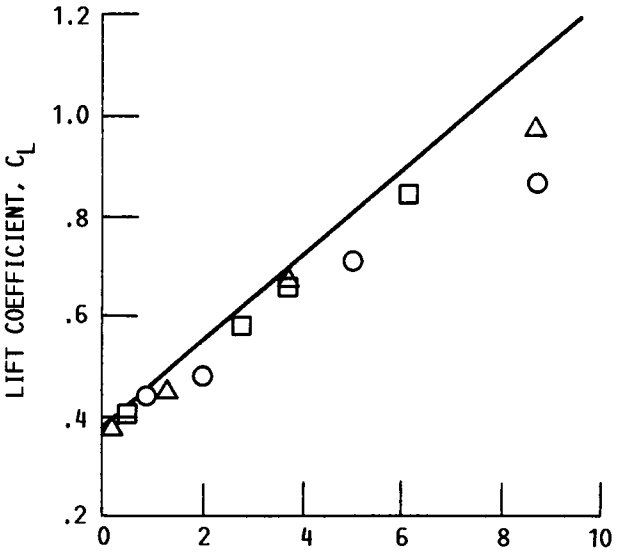

(A) VARIATION OF AIRCRAFT C_L VERSUS α.

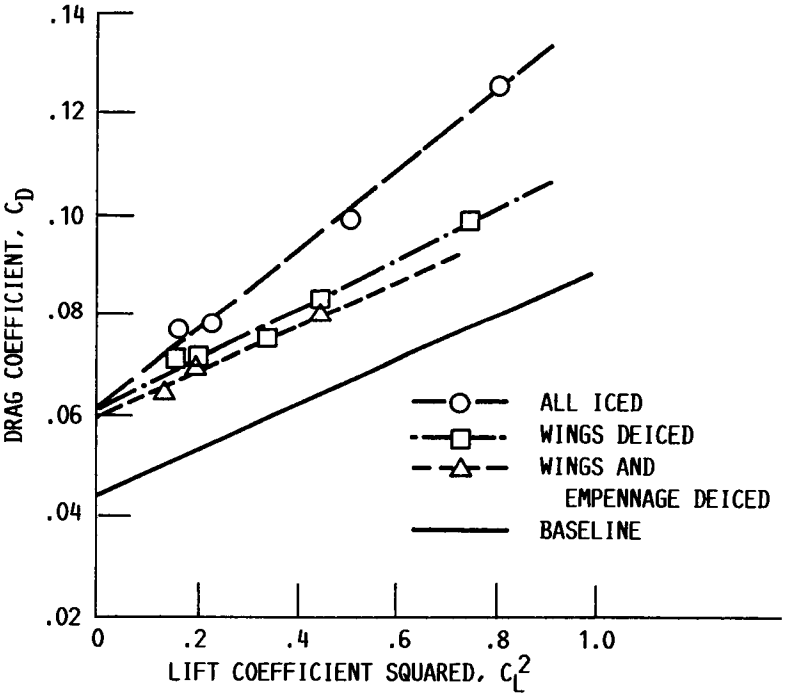

(B) SHIFT IN AIRCRAFT DRAG POLAR.

FIGURE 24. - EFFECT OF GLAZE ICE ON AIRCRAFT LIFT CURVE AND DRAG POLAR; FLIGHT 83-10.

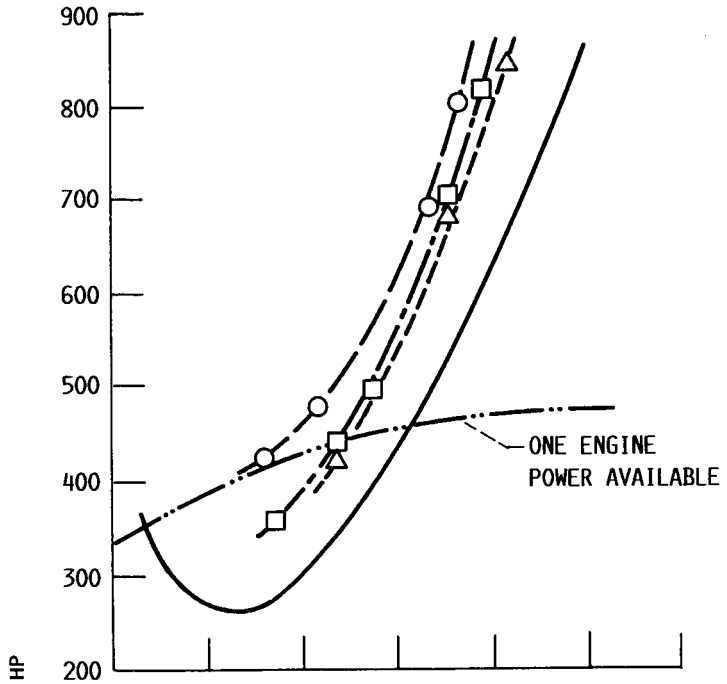

(A) FLIGHT TEST DATA CORRECTED TO STANDARD DAY, SEAL LEVEL, AND STANDARD WEIGHT CONDITIONS.

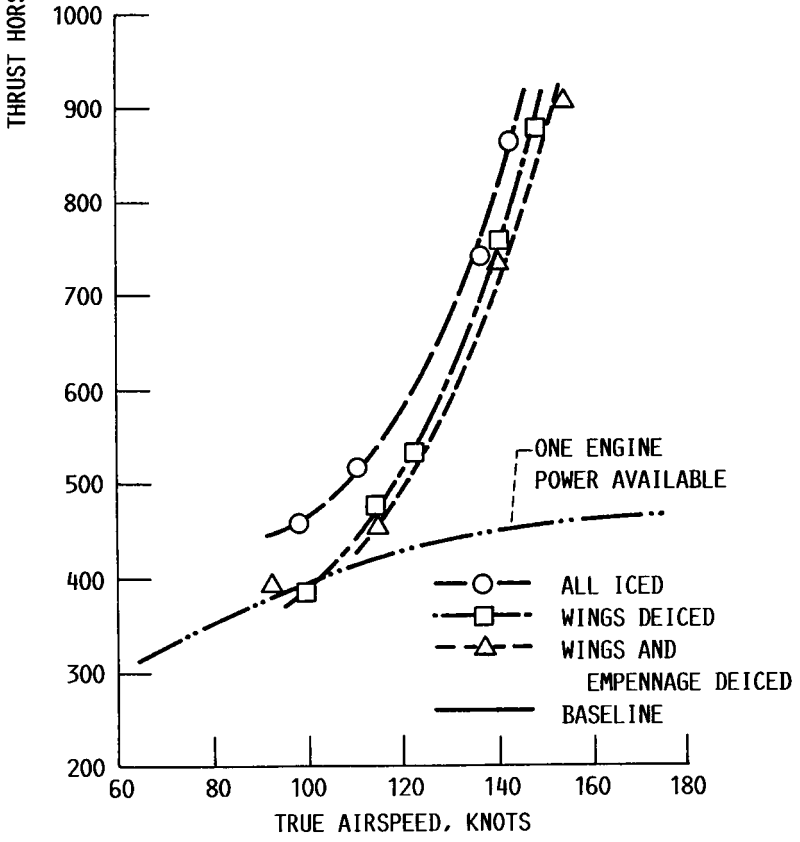

(B) TEST CONDITIONS AT 6000 FT FLIGHT TEST DATA CORRECTED TO STANDARD WEIGHT ONLY.

FIGURE 25. - EFFECT OF GLAZE ICE ON POWER REQUIRED COMPARED TO ONE ENGINE POWER AVAILABLE; FLIGHT 83-10.

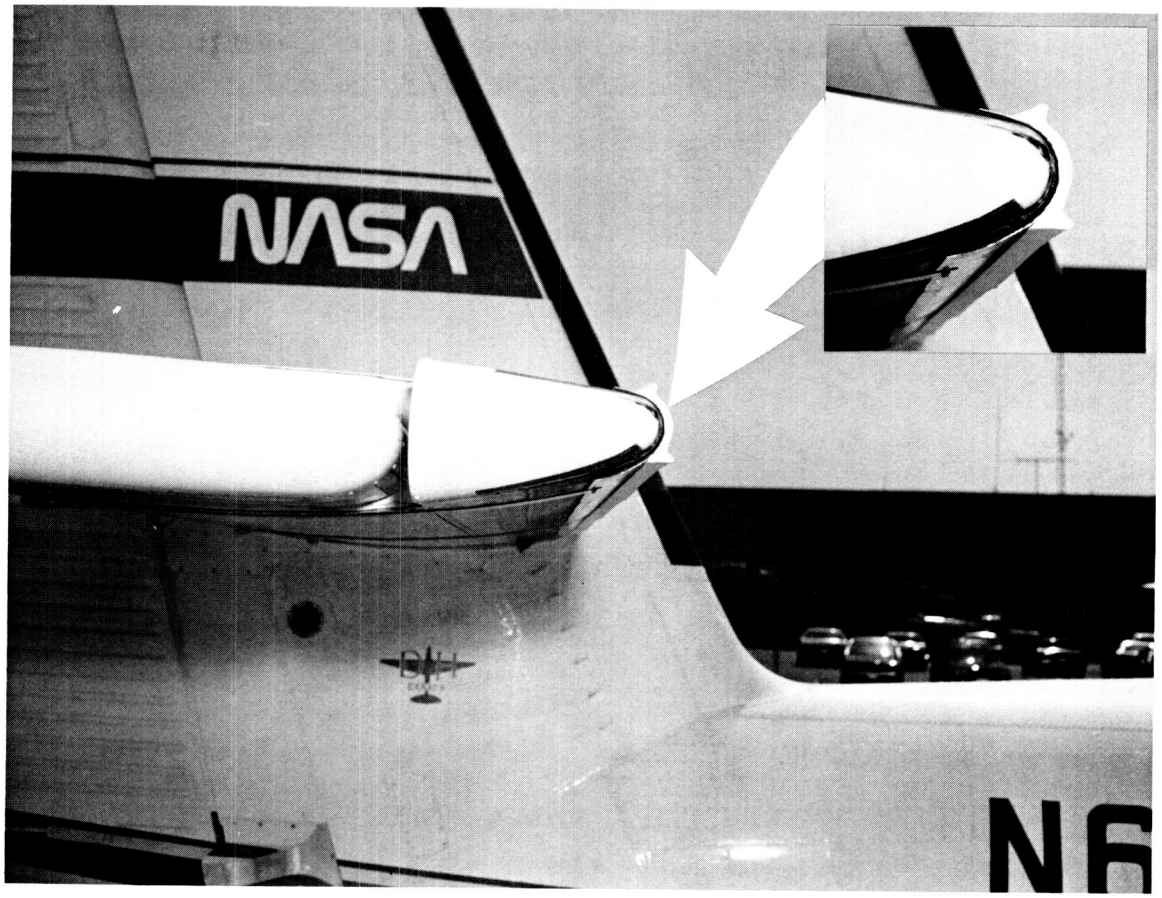

FIGURE 26. - 'STYROFOAM ICE' BONDED TO LEADING EDGE OF HORIZONTAL TAIL.

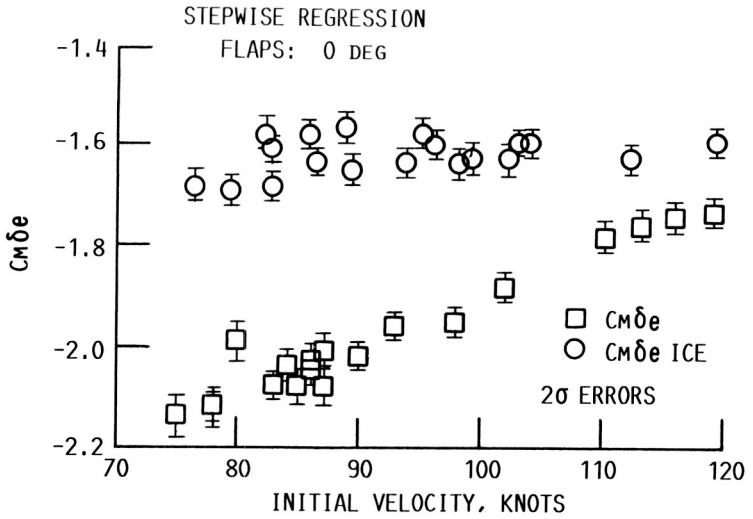

FIGURE 27. - DEGRADATION OF ELEVATOR CONTROL POWER AS MEASURED BY MSR ANALYSIS FOR 'STYROFOAM ICE' ON HORIZONTAL TAIL.

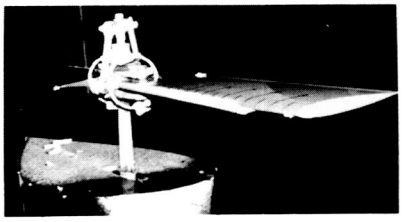

ICED OH-58 TAIL ROTOR RIG IN IRT

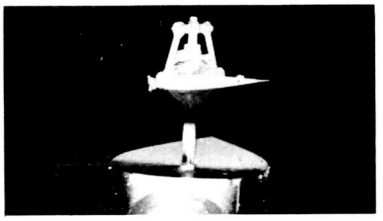

END VIEW OF TYPICAL OH-58 ROTOR BLADE ICE SHAPE

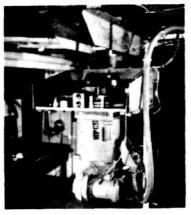

OH-58 TAIL ROTOR RIG DRIVE SYSTEM

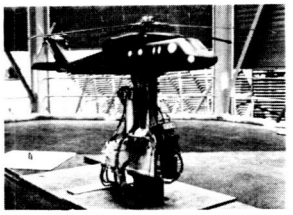

NEXT ROTOR TEST IN IRT: SIKORSKY POWERED FORCE MODEL WITH 6-COMPONENT INTERNAL FORCE BALANCE

FIGURE 28. - ROTORCRAFT ICING TESTS IN NASA IRT.

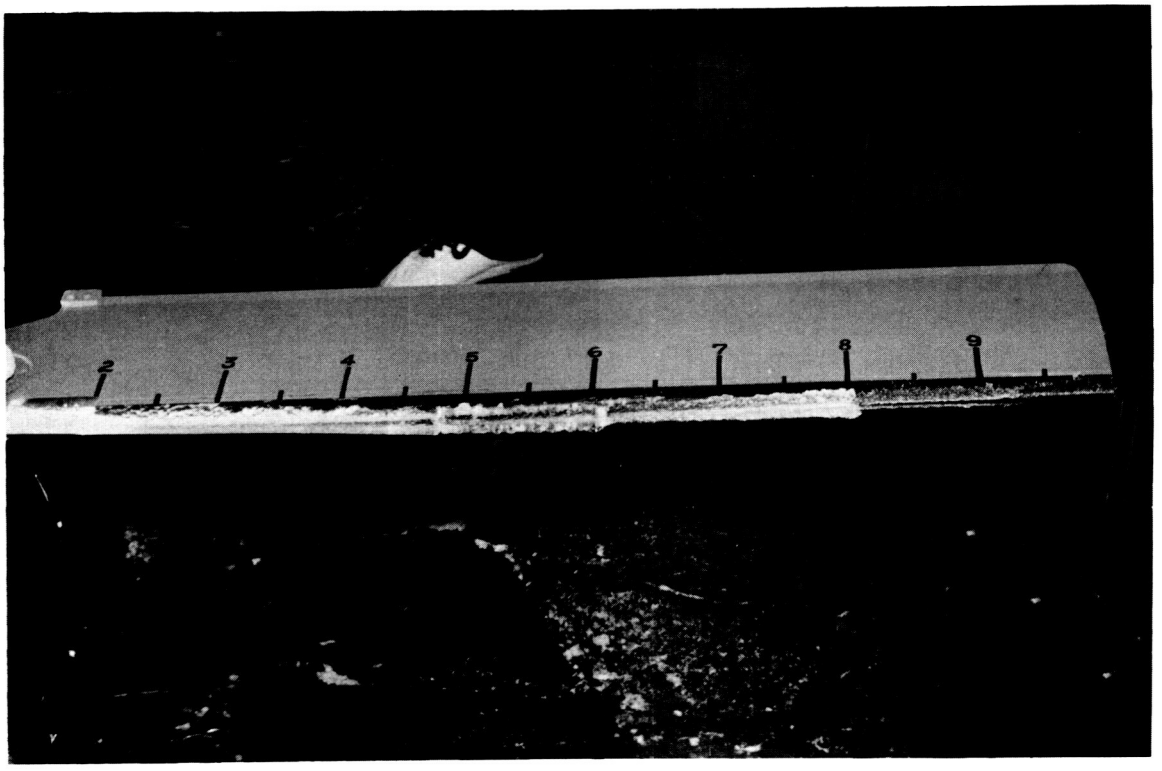

FIGURE 29. - ICE ACCRETION ALONG SPAN OF OH-58 TAIL ROTOR.

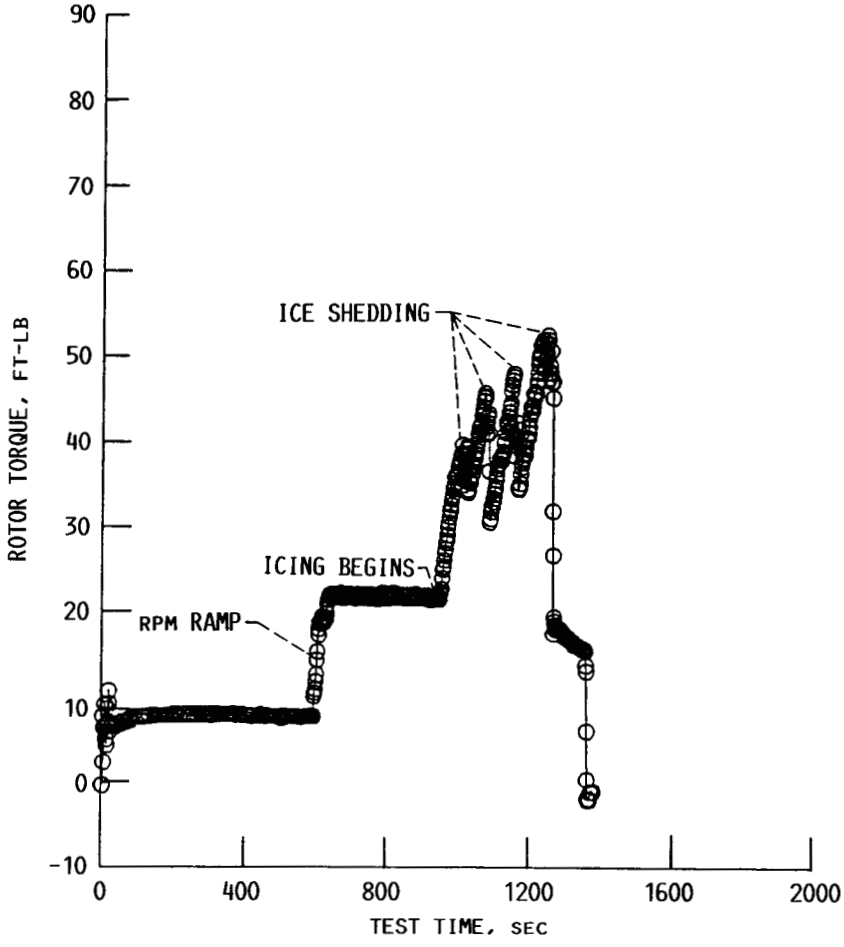

FIGURE 30. - OH-58 ROTOR TORQUE VARIATION WITH TIME DURING ICING TEST IN THE NASA IRT.

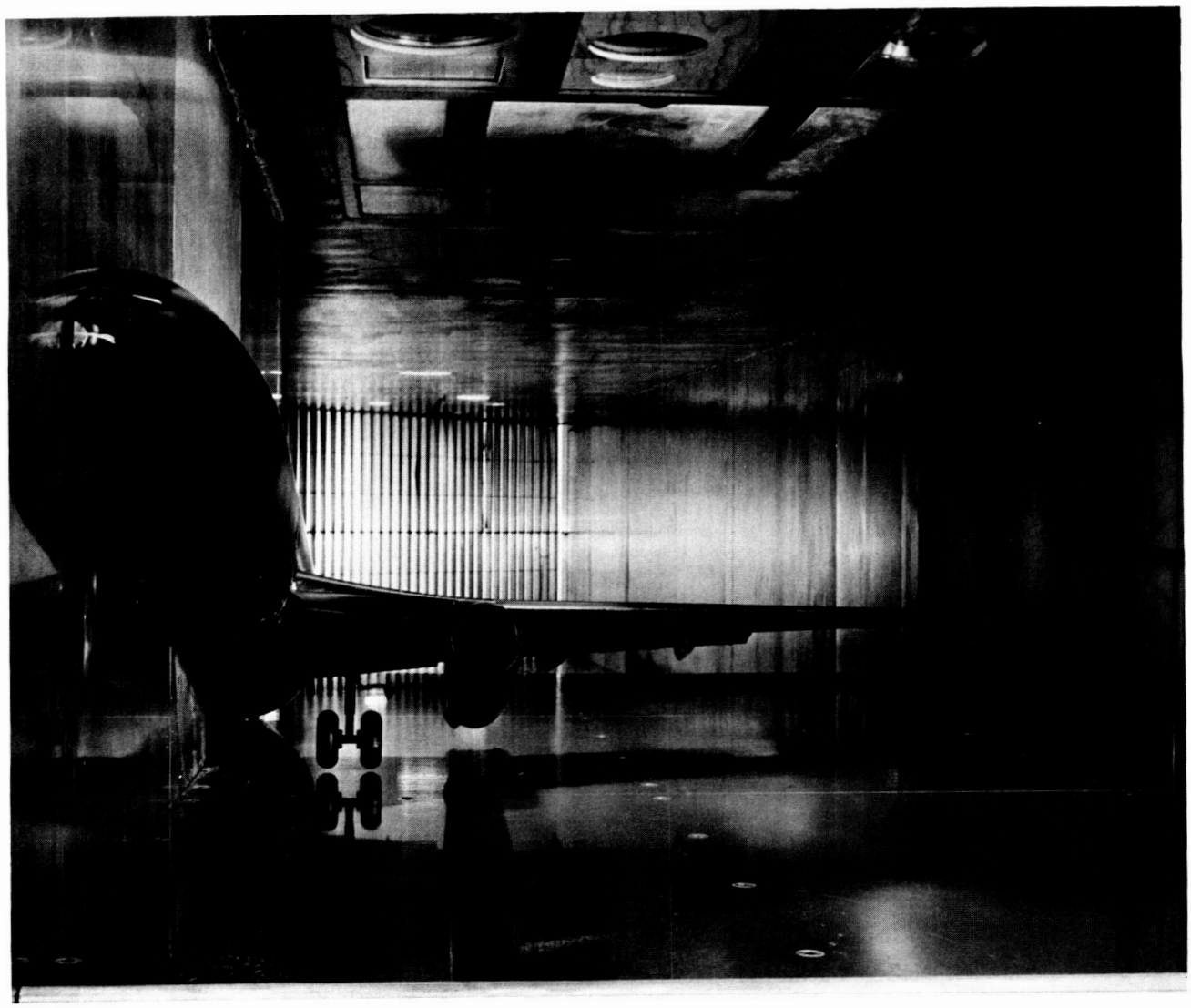

FIGURE 31. - BOEING 737-200 ADV HALF MODEL WITH GROUND PLANE, INSTALLED IN NASA IRT.

FIGURE 32. - FRONT VIEW OF 2D AIRFOIL MODEL (BOEING 737-200 ADV) INSTALLED BETWEEN SPLITTER WALLS IN NASA IRT.

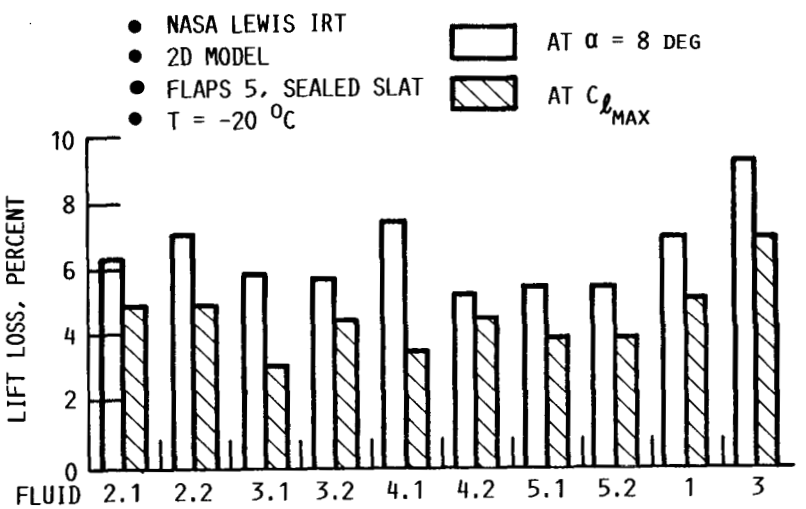

FIGURE 33. - LIFT LOSS OF EXPERIMENTAL TYPE II GROUND DEICING FLUIDS COMPARED WITH ORIGINAL TYPE I (1) AND TYPE II (3) FLUIDS.

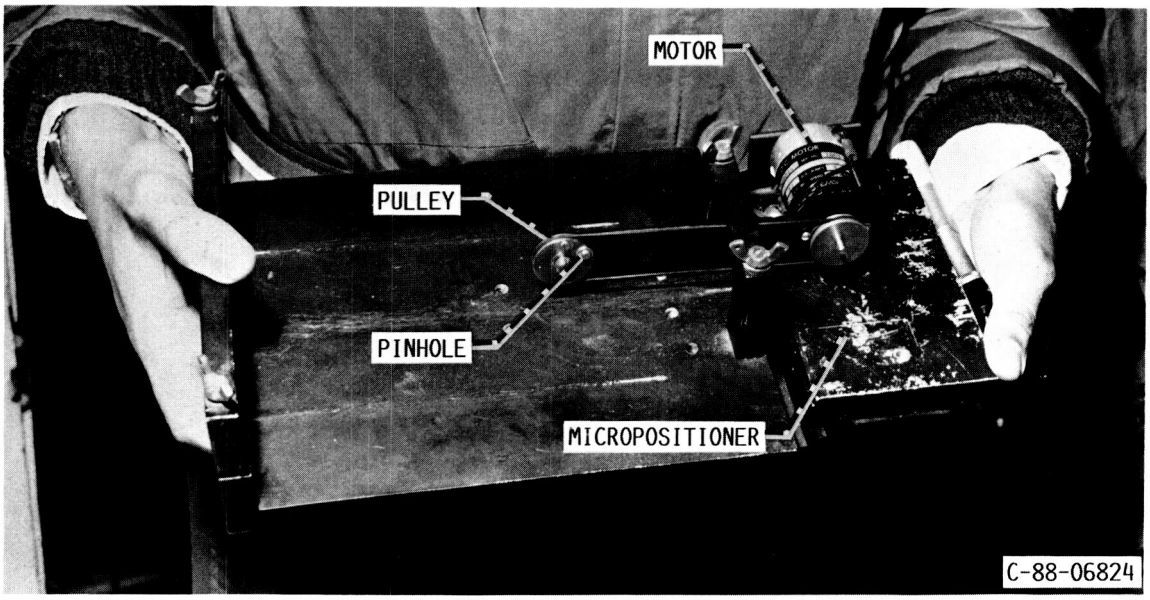

(A) COMPONENTS OF THE CALIBRATOR.

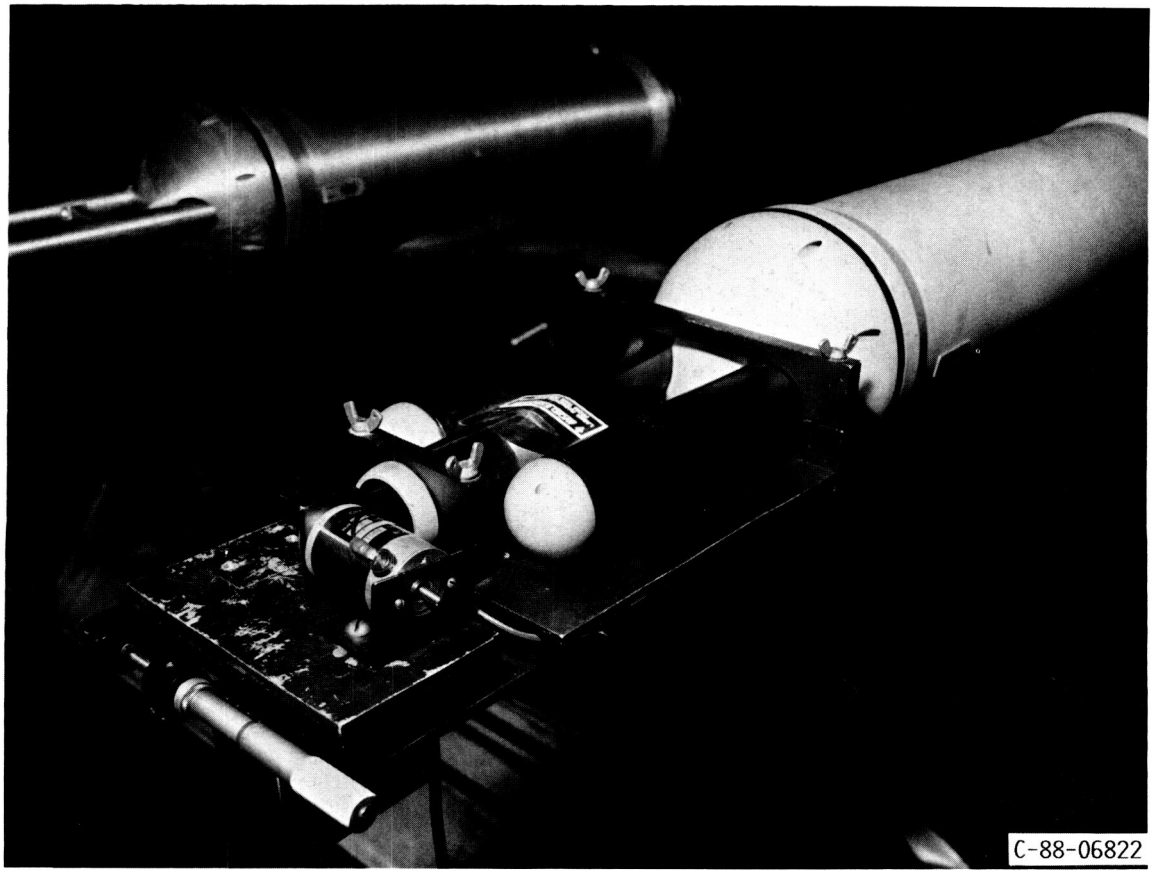

(B) CALIBRATOR ATTACHED TO FSSP.

FIGURE 34. - ROTATING PINHOLE CALIBRATOR.

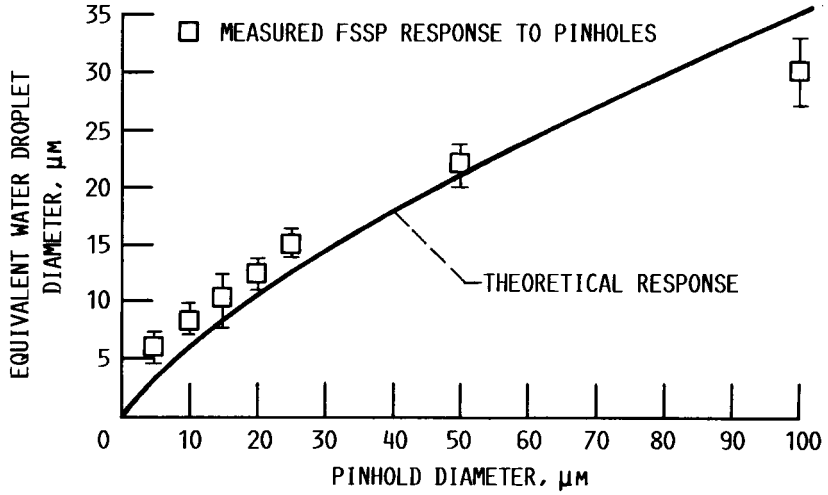

FIGURE 35. - CALIBRATION OF FSSP USING ROTATING PINHOLES.

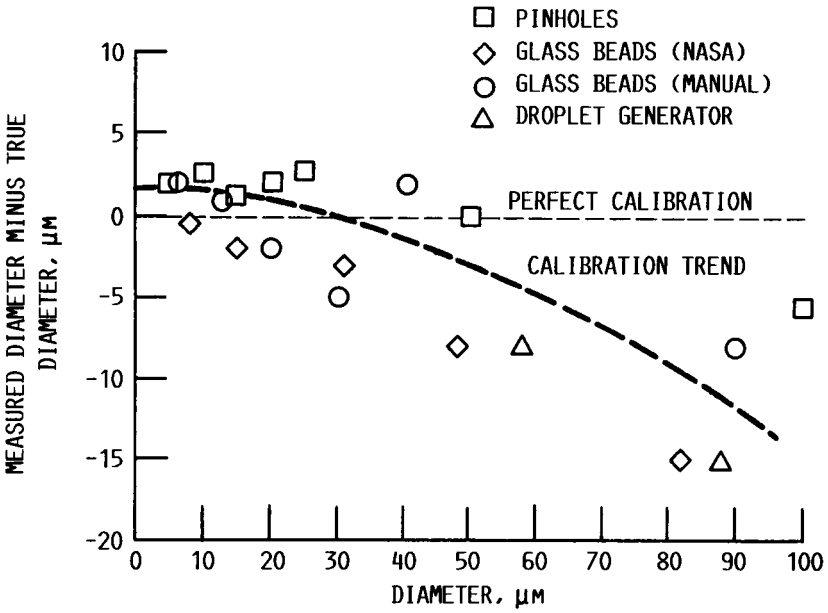

FIGURE 36.- CALIBRATION ACCURACY OF THE EXTENDED-RANGE FSSP.

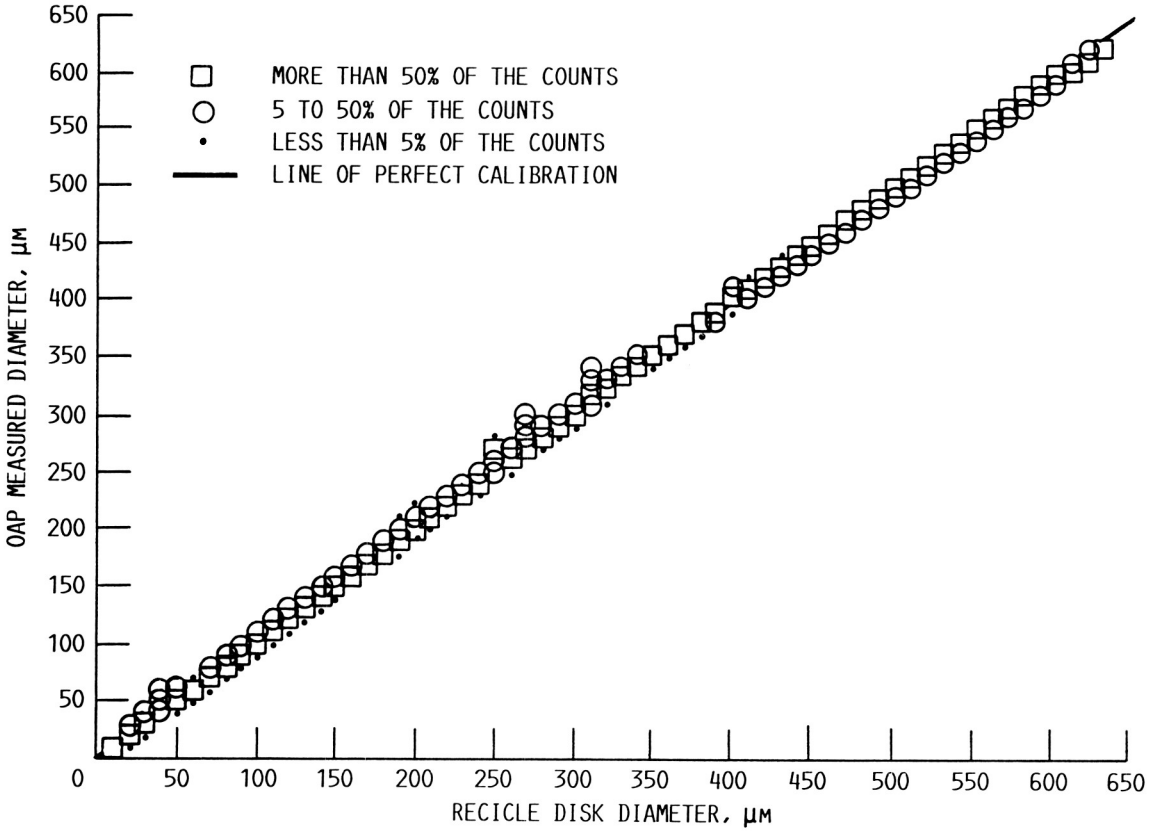

FIGURE 37. - CALIBRATION CURVE FOR THE OAP USING THE ROTATING RETICLE.

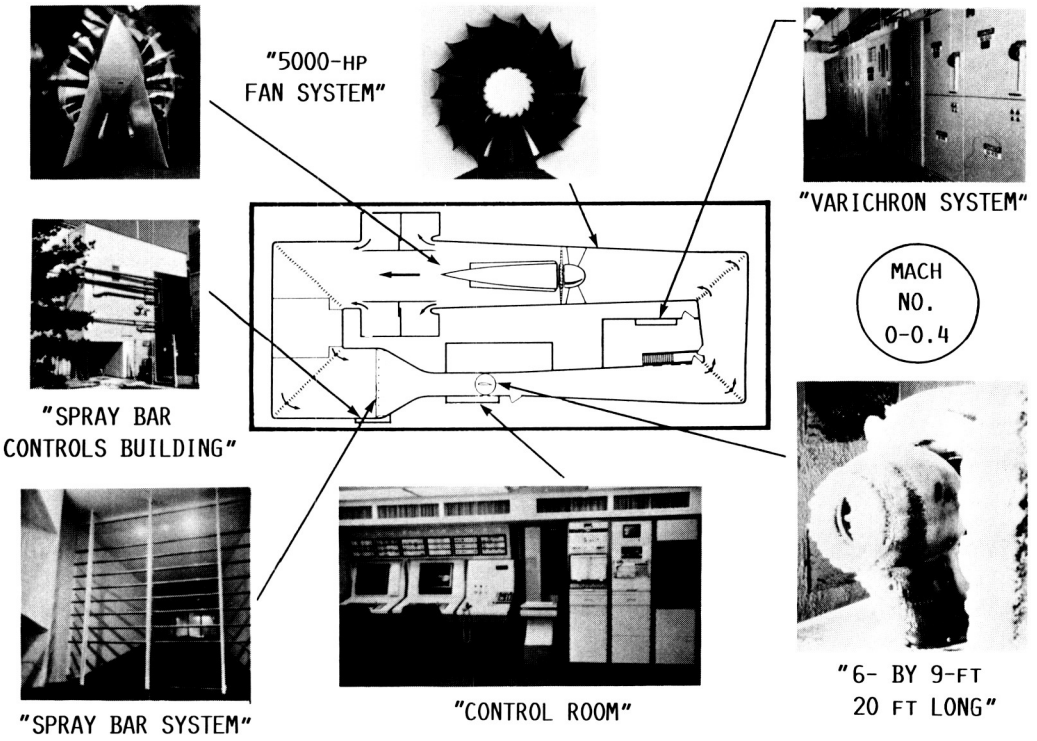

FIGURE 38. - SCHEMATIC OF NASA ICING RESEARCH TUNNEL FLOW CIRCUIT.

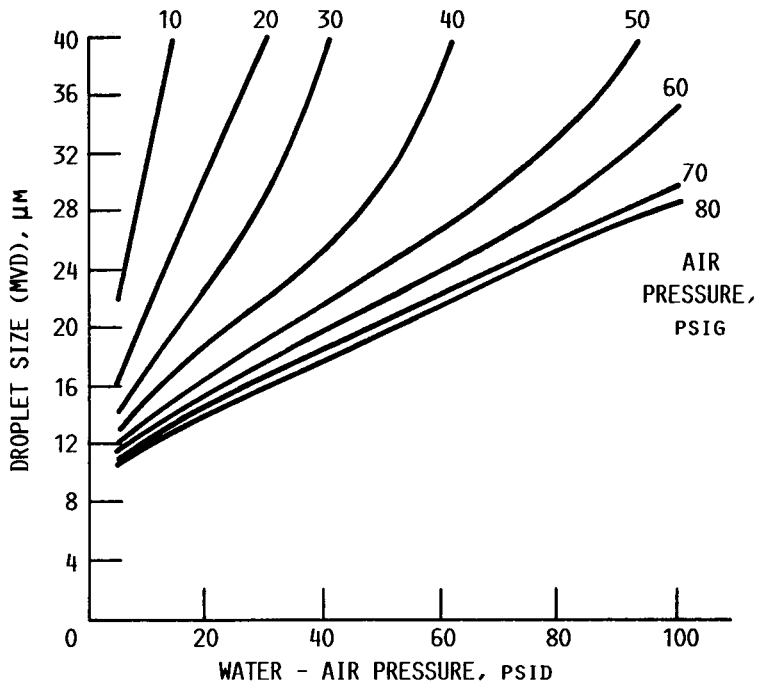

FIGURE 39. - DROPLET SIZE CALIBRATION FOR STANDARD NOZZLES IN NASA IRT.

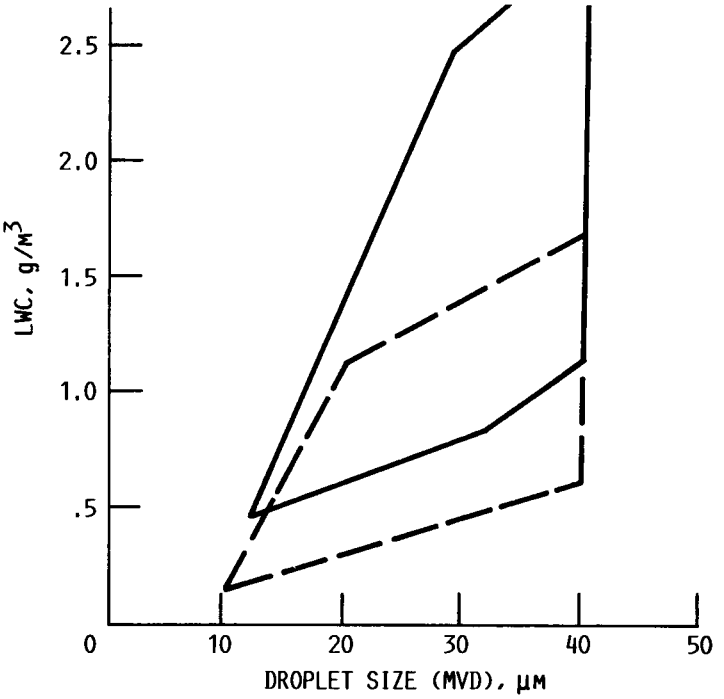

FIGURE 40. - OPERATING ENVELOPE FOR THE NASA IRT CLOUD AT 250 MPH.

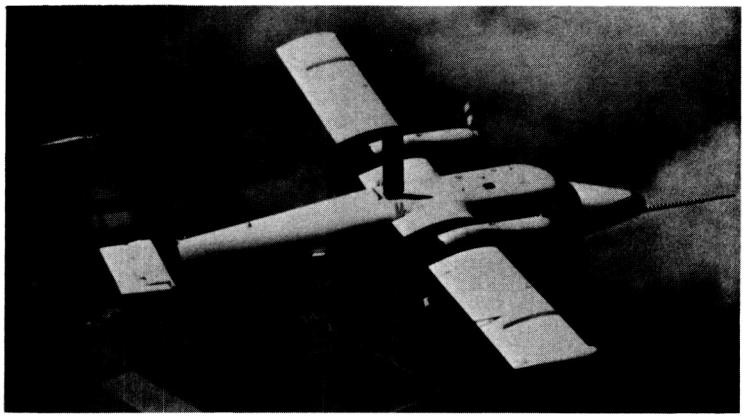

FIGURE 41. - AIRFOIL WITH HEAT TRANSFER GAUGES SHOWN MOUNTED ON THE TWIN OTTER.

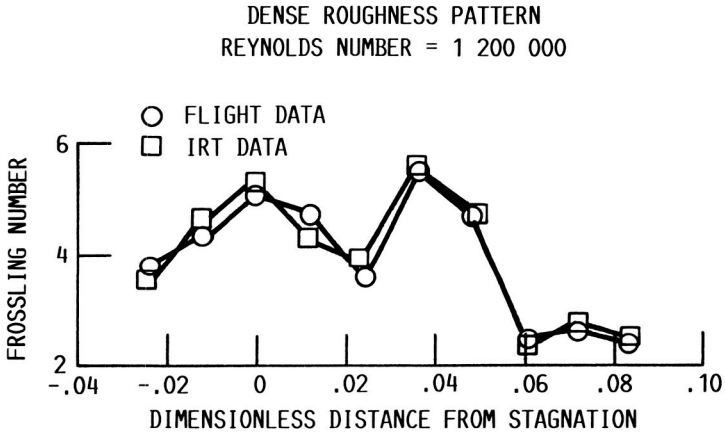

FIGURE 42. - COMPARISON OF HEAT TRANSFER BETWEEN FLIGHT AND NASA IRT.

NASA
National Aeronautics and Space Administration

Report Documentation Page

1. Report No.	2. Government Accession No.	3. Recipient's Catalog No.
NASA TM-101989		

4. Title and Subtitle
NASA's Program on Icing Research and Technology

5. Report Date

6. Performing Organization Code

7. Author(s)
John J. Reinmann, Robert J. Shaw, and Richard J. Ranaudo

8. Performing Organization Report No.
E-4692

10. Work Unit No.
505-68-11

9. Performing Organization Name and Address
National Aeronautics and Space Administration
Lewis Research Center
Cleveland, Ohio 44135-3191

11. Contract or Grant No.

13. Type of Report and Period Covered
Technical Memorandum

12. Sponsoring Agency Name and Address
National Aeronautics and Space Administration
Washington, D.C. 20546-0001

14. Sponsoring Agency Code

15. Supplementary Notes
Prepared for the Symposium on Flight in Adverse Environmental Conditions sponsored by the Flight Mechanics Panel (FMP) of AGARD, Gol, Norway, May 8-12, 1989.

16. Abstract

This paper reviews NASA's program in aircraft icing research and technology. The program relies heavily on computer codes and modern applied physics technology in seeking icing solutions on a finer scale than those offered in earlier programs. Three major goals of this program are (1) to offer new approaches to ice protection, (2) to improve our ability to model the response of an aircraft to an icing encounter, and (3) to provide improved techniques and facilities for ground and flight testing. This paper reviews the following program elements: (1) new approaches to ice protection; (2) numerical codes for deicer analysis; (3) measurement and prediction of ice accretion and its effect on aircraft and aircraft components; (4) special wind tunnel test techniques for rotorcraft icing; (5) improvements of icing wind tunnels and research aircraft; (6) ground de-icing fluids used in winter operation; (7) fundamental studies in icing; and (8) droplet sizing instruments for icing clouds.

17. Key Words (Suggested by Author(s))	18. Distribution Statement
Aircraft icing	Unclassified – Unlimited Subject Category 01

19. Security Classif. (of this report)	20. Security Classif. (of this page)	21. No of pages	22. Price*
Unclassified	Unclassified	54	A04

NASA FORM 1626 OCT 86

*For sale by the National Technical Information Service, Springfield, Virginia 22161